UNIVERZA V LJUBLANI
FAKULTETA ZA FARMACIJO

MATIC DOLINAR

MAGISTRSKO DELO

ENOVITI MAGISTRSKI ŠTUDIJ FARMACIJE

Ljubljana, 2018

UNIVERZA V LJUBLANI
FAKULTETA ZA FARMACIJO

MATIC DOLINAR

RAZVOJ IN VREDNOTENJE HITOSANSKIH NANODELCEV Z VGRAJENIMI FLUORIDI ZA DENTALNO UPORABO

DEVELOPMENT AND CHARACTERIZATION OF FLUORIDE-LOADED CHITOSAN NANOPARTICLES FOR DENTAL APPLICATION

Ljubljana, 2018

Master's thesis was written based on research work done from September 2016 to December 2016 at the School of Pharmacy, University of Oslo, Norway, under co-mentorship of Professor Doctor Marianne Hiorth and mentorship of Associate Professor Doctor Petra Kocbek.

ACKNOWLEDGEMENTS

First and foremost, I want to express my sincere gratitude to Professor Doctor Marianne Hiorth and Associate Professor Doctor Sanko Hoan Nguyen. Thank you for giving me the opportunity to be a part of your wonderful research group, for your kind guidance and professional supervision, for sharing your endless knowledge and experience, and the encouragement and trust I received.

I am thankful to my mentor Associate Professor Doctor Petra Kocbek for all her mentorship, assistance, support, and effort with helping me write this master's thesis.

I would like to express my gratitude to the lab technician Tove Larsen for her generous help in the laboratory, and to Sara Pistone for sharing some hidden insights from her work with me. Sara, this helped me immensely.

My appreciation goes to Camila Bui for spending sometimes uncomfortably long days in the lab with me while working on the research work for her thesis. Camila, it would not have been the same without you and your music.

Last but not least, I would like to thank my dear family for unconditional support and motivation throughout the years, and to my friends scattered all around the globe for always believing in me.

STATEMENT

I hereby declare that this master's thesis was done by me under supervision of Associate Professor Doctor Petra Kocbek and co-supervision of Professor Doctor Marianne Hiorth.

Matic Dolinar

COMMITTEE

Head of Committee: Associate Professor Doctor Anamarija Zega

Mentor: Associate Professor Doctor Petra Kocbek

Co-mentor: Professor Doctor Marianne Hiorth

Member of Committee: Assistant Doctor Nejc Horvat

TABLE OF CONTENTS

LIST OF FIGURES

LIST OF TABLES

LIST OF EQUATIONS

POVZETEK

Ustne bolezni predstavljajo enega izmed večjih zdravstvenih bremen modernega časa, pri čemer se z zobno gnilobo spopada skoraj celotna odrasla populacija na svetovni ravni. Prosti sladkorji, prisotni v sodobni hrani, so najpomembnejši s prehrano povezani dejavnik, ki je vpleten v začetek razvoja zobne gnilobe. Zagotavljanje ustrezne ustne higiene in zdravja ustne votline je cilj razvoja sodobnih pristopov in dostavnih sistemov za preprečevanje in zdravljenje kariesa, s ciljem zmanjšati negativne posledice ustnih bolezni.

V sklopu raziskav tega magistrskega dela smo izdelali hitosanske nanodelce z vgrajenimi fluoridi, ki so zaradi protibakterijskega učinka najučinkovitejše sredstvo proti zobni gnilobi. Za izdelavo nanodelcev smo izbrali hitosan, ki je najbolj raziskan bioadheziven polisaharid, združljiv z biološkim okoljem. Nanodelce smo pripravili z metodo ionotropnega geliranja in jih označili s fluorescentnim barvilom.

Ugotovili smo, da je gelska filtracija ustrezna metoda za ločevanje nanodelcev od prostih molekul. S to metodo smo učinkovito odstranili nevezano fluorescentno barvilo, proste molekule polimera, nevgrajene fluoridne ione in morebiti prisotne nečistoče.

Raziskali smo stabilnost hitosanskih nanodelcev v prisotnosti umetne sline (uporabili smo SAGF medij), da bi ugotovili, kako prisotnost sestavin v slini vpliva na zgradbo in obnašanje nanodelcev. Raziskava je pokazala, da v umetni slini prihaja do združevanja in nato do razpada nanodelcev.

Da bi ugotovili, ali imajo hitosanski nanodelci z vgrajenimi fluoridi sposobnost vezave na površino zobne sklenine, smo proučili vezavo omenjenih nanodelcev na hidroksiapatit. Kalcijev hidroksiapatit smo uporabili kot modelno snov za posnemanje zobne sklenine, ker izkazuje podobne površinske lastnosti. Rezultati so pokazali, da imajo hitosanski nanodelci sposobnost vezave na površino uprašenega hidroksiapatita.

Izvedli smo tudi raziskavo vezave hitosanskih nanodelcev na mucine. Ugotovili smo, da prihaja do interakcij med hitosanskimi nanodelci in mucini, a se odstotek nanodelcev, vezanih na mucine, v proučevanem koncentracijskem območju mucinov ni spreminjal z njihovo koncentracijo v disperziji nanodelcev.

Na podlagi rezultov lahko zaključimo, da imajo hitosanski nanodelci z vgrajenimi fluoridi lastnosti, ki kažejo, da bi lahko postali v prihodnosti učinkovito sredstvo za preprečevanje in zdravljenje zobne gnilobe ter drugih bolezni zob in obzobnih tkiv.

Ključne besede: hitosanski nanodelci • ionotropno geliranje • zobna gniloba • hidroksiapatit • umetna slina

ABSTRACT

Oral diseases represent one of the major health burdens in modern days with dental caries present in nearly 100 % of adult population in majority of countries worldwide. Free sugars present in modern foods are the main dietary factor contributing towards its development. The research and development of novel advanced pharmaceutical systems for oral hygiene is thus essential to minimize occurrence, the ramifications and the impact of oral diseases.

The nanodelivery system investigated in scope of this master's thesis were chitosan nanoparticles loaded with fluoride as the most effective anti-caries agent with potent antibacterial activity. Chitosan was chosen as one of the most widely investigated polysaccharides due to its biocompatibility, biodegradability, bioadhesive properties and nontoxicity. The chitosan nanoparticles were prepared by ionotropic gelation and labeled with fluorescent dye.

Furthermore, gel-filtration was shown to be suitable separation and purification method due to its efficacy in separation of fluoride-loaded nanoparticles from free molecules.

Interaction studies of nanoparticles with artificial salivary fluid (the SAGF medium) were performed in order to investigate how the presence of salivary components affects the structure and behavior of nanoparticles. The research showed the occurrence of nanoparticle aggregation and later disintegration with time in the salivary environment.

Moreover, the adhesion capacity of fluoride-loaded nanoparticles onto hydroxyapatite was investigated. Calcium hydroxyapatite was used as a model substance for dental enamel in research of bioadhesion because it displays similar surface characteristics as the dental enamel. The results revealed that chitosan nanoparticles had the ability to adhere onto hydroxyapatite powder.

An interaction study of chitosan nanoparticles with mucins was performed in order to investigate possible interactions. The results showed nanoparticles interacted with mucins, while the percentage of nanoparticles adsorbed onto mucins did not change significantly with respect to increasing amount of mucins added to nanoparticulate dispersion.

Based on the results it can be concluded that fluoride-loaded chitosan nanoparticles have characteristics that show that, in the future, they could become an effective agent in preventing and treating tooth decay and other diseases of teeth and periodontal tissues.

Keywords: chitosan nanoparticles • ionotropic gelation • tooth decay • hydroxyapatite • artificial saliva

RAZŠIRJENI POVZETEK

Ustne bolezni predstavljajo enega izmed večjih zdravstvenih bremen modernega časa, pri čemer se z zobno gnilobo spopada od šestdeset do devetdeset odstotkov šoloobveznih otrok in skoraj celotna odrasla populacija na svetovni ravni. V razvitih državah je pet do deset odstotkov sredstev iz zdravstvenega proračuna namenjenih zdravljenju zobne gnilobe, ki je eden izmed poglavitnih razlogov za sprejem otrok v bolnišnico v nekaterih državah z visokimi osebnimi prihodki. Prosti sladkorji, prisotni v moderni prehrani, kot so sladke pijače, torte, piškoti, bonboni, sirupi, med, sladkane žitarice in druge sladice, so prehranski dejavnik, ki povzroča začetek razvoja zobne gnilobe. Napredovala oblika zobne gnilobe ima lahko resne posledice na posameznikovo kakovost življenja, saj lahko povzroči pomanjkanje spanja, zaplete pri prehranjevanju, kronično bolečino ali se celo razvije v kronično sistemsko okužbo. Vse to kaže na velike potrebe po vlaganju v raziskave in razvoj naprednih formulacij za zagotavljanje ustrezne ustne higiene s ciljem zmanjšati negativne posledice ustnih bolezni.

V sklopu raziskav tega magistrskega dela smo izdelali hitosanske nanodelce z vgrajenimi fluoridi kot najučinkovitejšimi sredstvi proti zobni gnilobi z močnim protibakterijskim učinkom. Hitosan smo izbrali kot najbolj raziskan polisaharid zaradi njegove združljivosti z biološkim okoljem, sposobnosti bioadhezije in netoksičnosti. Poleg tega hitosanski nanodelci izkazujejo protivnetno in protibakterijsko delovanje. Fluor je ena izmed glavnih sestavin v skoraj vseh komercialno dostopnih zobnih pastah. Odlikuje ga sposobnost prehoda v pore zobne sklenine, s čimer okrepi površino zob in jo naredi odpornejšo na padce pH, ki so posledica zaužitja hrane, kar zmanjšuje verjetnost nastanka zobne gnilobe.

Hitosanske nanodelce z vgrajenimi fluoridi smo uspešno pripravili z metodo ionotropnega geliranja in jih označili s fluorescentnim barvilom fluorescein izotiocianat. Kot premreževalo smo uporabili natrijev tripolifosfat in kot disperzni medij prečiščeno vodo. Končna disperzija nanodelcev je vsebovala 0,070 % (m/m) hitosana in 0,2 % (m/m) natrijevega fluorida. Razmerje med hitosanom in natrijevim tripolifosfatom je bilo 80:20 (m:m). Delci so bili velikosti ~100 nm s homogeno porazdelitvijo velikosti.

Ugotovili smo, da je gelska filtracija ustrezna metoda za ločevanje nanodelcev od prostih molekul. Ločevanje poteka, ko molekule ali delci potujejo skupaj z mobilno fazo skozi porozni medij, do katerega imajo različen dostop zaradi steričnih vplivov: manjše molekule lahko vstopijo v pore, medtem ko je vstop večjim molekulam in delcem

onemogočen, zaradi česar se večje molekule krajši čas zadržijo v koloni. S to metodo smo učinkovito odstranili nevezano fluorescentno barvilo, proste molekule polimera, nevgrajene fluoridne ione in morebiti prisotne nečistoče.

Raziskali smo stabilnost hitosanskih nanodelcev v prisotnosti umetne sline, da bi ugotovili, kako prisotnost sestavin v slini vpliva na zgradbo in obnašanje nanodelcev. Kot umetno slino smo uporabili SAGF medij s pH 6,8. Ugotovili smo, da v okolju s slino prihaja do združevanja in kasneje razpadanja nanodelcev s časom. Ionska moč, pH sline in elektroliti v njej vplivajo na stabilnost disperzije nanodelcev. Nasprotno imajo nabiti multivalentni ioni v slini (karbonati, sulfati, fosfati) sposobnost tvorjenja ionskih vezi med nanodelci, kar vodi v njihovo združevanje in nastanek skupkov. Poleg tega lahko vezava anionov sline na posamezne pozitivno nabite polimerne verige nanodelcev zmanjša celokupni naboj nanodelcev, kar lahko prav tako spodbuja njihovo združevanje. Razpad nanodelcev lahko nastopi kot posledica prekinitve elektrostatičnih vezi med polimerom (hitosan) in premreževalom (natrijev tripolifosfat).

Da bi ugotovili, ali imajo hitosanski nanodelci z vgrajenimi fluoridi sposobnost vezave na površino zobne sklenine, smo proučili vezavo omenjenih nanodelcev na hidroksiapatit. Kalcijev hidroksiapatit smo uporabili kot modelno snov za posnemanje zobne sklenine, ker izkazuje podobne površinske lastnosti. Hidroksiapatit ima zaradi svoje amfoterne narave sposobnost tvorjenja povezav s kationi in anioni odvisno od pH medija, v katerem se nahaja. Proces adsorpcije in desorpcije vključuje dve različni vezavni mesti, ki ju ima hidroksiapatit: pozitivno nabite kalcijeve ione (Ca^{2+}) in negativno nabite fosfatne ione (PO_4^{3-}). Obe vezavni mesti tvorita močne nespecifične elektrostatske interakcije z nasprotno nabitimi ioni. Adsorpcija nanodelcev je odvisna ravnotežja med privlačnimi in odbojnimi silami med nanodelci in površino hidroksiapatita, na katere vpliva pH, ionska moč in koncentracija različnih ionov, prisotnih v okolici. Rezultati so pokazali, da imajo hitosanski nanodelci sposobnost vezave na površino uprašenega hidroksiapatita, pri čemer se odstotek adsorpcije nanodelcev veča z maso hidroksiapatita, dokler ne doseže vrednosti, pri kateri so vsi nanodelci vezani na površino hidroksiapatita.

Med drugim smo raziskali tudi vpliv sprememb pH disperznega medija na fluorescenco uporabljenega fluorescentnega barvila fluorescein izotiocianat. Izkazalo se je, da alkalnost medija spodbuja močno fluorescenco, medtem ko zmanjšanje pH medija zmanjša intenziteto fluorescence. To je posledica različnih protolitičnih oblik, odvisnih od pH

medija, v katerem se nahaja fluorescein izotiocianat. Domnevno se le-ta glede na pH lahko nahaja v obliki kationa, nevtralne molekule, laktona ali monoaniona in dianiona.

Izvedli smo tudi raziskavo vezave hitosanskih nanodelcev na mucine. Ugotovili smo, da prihaja do interakcij med hitosanskimi nanodelci in mucini, a se odstotek nanodelcev, vezanih na mucine, ni spreminjal s koncentracijo mucionov v disperziji nanodelcev. Domnevno se lahko več kot ena molekula mucinov veže na molekulo hitosana, zaradi česar bi lahko bil odstotek vezave nanodelcev na mucine neodvisen od koncentracije mucinov. Do povezave pride med pozitivnimi amino skupinami hitosana in ostanki sialične kisline pri mucinih. Da je mukoadhezija uspešna, mora priti do prepletanja in prodiranja polimernih verig hitosana v razvejano strukturo mucinov. Interakcije med nanodelci in mucini so posledica van der Waalsovih privlačnih sil, elektrostatskih interakcij, vodikovih vezi in hidrofobnih interakcij.

Nanodelci, obravnavani v tem magistrskem delu, so vsekakor izkazali potencial, da bi lahko postali v prihodnosti učinkovito sredstvo za preprečevanje in zdravljenje zobne gnilobe ter drugih bolezni zob in obzobnih tkiv. V prihodnje je bistveno, da se natančno razišče njihova stabilnost v umetni oz. naravni slini, saj je le-ta bistvena za njihovo učinkovitost. Smotrno bi bilo raziskati in ovrednotiti tudi adhezijo nanodelcev na zobno sklenino v kislih pogojih, ki so *in vivo* posledica presnavljanja sladkorjev s strani kariogenih bakterij. Nanodelci, adsorbirani na površino zobne sklenine, bi naj okrepili tudi fizično pregrado na površini zoba, ki jo tvori pelikel, zato bi bilo smiselno proučiti tudi njihovo učinkovitost pri preprečevanju raztapljanja in erozije zobne sklenine v kislih pogojih. Med drugim bi bilo smiselno tudi raziskati vgrajevanje in učinkovitost dostave drugih zdravilnih učinkovin za zdravljenje ustnih bolezni s hitosanskimi nanodelci.

Področje nanodostavnih sistemov za uporabo v ustni votlini je izredno široko in nedvomno mnogo obeta, zato se v prihodnosti nadejamo številnih raziskav in novih odkritij, ki bi lahko izboljšala učinkovitost preprečevanja in zdravljenja ustnih bolezni.

LIST OF USED ABBREVIATIONS

API	Active pharmaceutical ingredient
DDS	Drug delivery system
DLS	Dynamic light scattering
FITC	Fluorescein isothiocyanate
FA	Fluoroapatite
GF	Gel-filtered
HA	Hydroxyapatite
NCD	Noncommunicable disease
NGF	Non-gel-filtered
NP	Nanoparticle
PDI	Polydispersity index
TPP	Tripolyphosphate
WHO	World Health Organization

1 INTRODUCTION

Oral diseases represent one of the major health burdens in all regions around the world. Despite great endeavors to reduce their dissemination, dental caries still affects 60–90 % of school-aged children in most industrialized countries and is found in nearly 100 % of adult population in majority of countries worldwide (1). It has been reported that its prevention and treatment consume 5–10 % of healthcare budgets in developed countries, while being one of the leading reasons for children hospitalization in some high-income countries (2). Free sugars present in sugar-sweetened beverages, 100 % fruit juices and other common sources of free sugars such as cakes, biscuits, sweet deserts, syrups, honey, and sweetened cereals are the main dietary factor contributing towards the development of dental caries. Severe dental caries can have serious ramifications on quality of life as it can cause sleep deprivation, eating complications, chronic pain, and may develop into chronic systemic infection (2).

If we want to reduce caries occurrence, it is imperative to reduce free sugars consumption population-wide as well as enhance and advance prevention approaches and their accessibility and availability (2). For this reason, the development of novel advanced pharmaceutical systems for oral hygiene is essential in order to minimize the true burden and the impact of oral diseases. Apart from this, a comprehensive patient-centered oral health care will play a major role in addressing public oral health issues worldwide.

1.1 Oral Cavity

The oral cavity (*Figure 1*) represents the first segment of gastrointestinal tract that receives food, produces saliva and holds an important role in communication, respiration, and food and drink consumption.

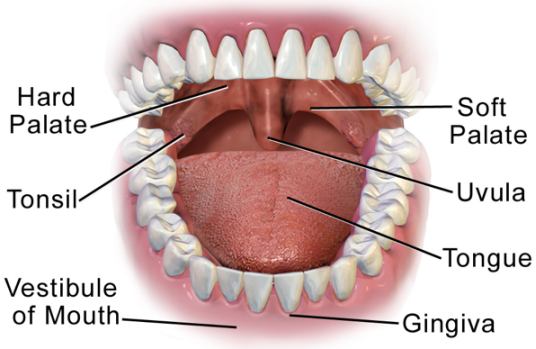

***Figure 1**: The anatomy of the oral cavity (3).*

The oral cavity is lined with a mucous membrane and comprised of two main regions: the vestibule and the oral cavity proper. The vestibule of mouth lies between the teeth, lips and cheeks, whereas the oral cavity proper encompasses the area enclosed anteriorly and laterally by the teeth and gingiva, superiorly by the palate, inferiorly by the tongue and the floor of the mouth, and posteriorly by the opening into the pharynx (4).

In the beginning of growth development, humans grow 20 primary teeth, commonly referred to as milk teeth or baby teeth, that are later naturally eliminated and replaced by 32 permanent teeth (4).

1.1.1 Dental Enamel

The dental enamel is the hardest substance in human body covering the surface of the tooth crown as displayed in *Figure 2*. Enamel is an acellular tissue composed of 88–90 % inorganic mineral calcium hydroxyapatite (HA), $Ca_{10}(PO_4)_6(OH)_2$, arranged in long and thin crystals, with organic material and water being the remainder (4, 5).

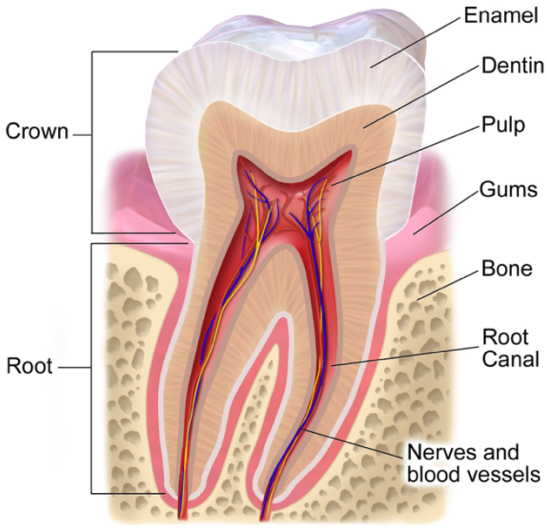

***Figure 2**: The anatomy of a human tooth (6).*

The solubility of enamel changes depending on the composition of the liquid with which it interacts. To be more specific, the fluid present in its microenvironment directly affects the equilibrium between the HA and its ions in solution, as represented in *Equation 1*.

$$Ca_{10}(PO_4)_6(OH)_2 \underset{\text{mineralization}}{\overset{\text{demineralization}}{\rightleftharpoons}} 10Ca^{2+} + 6PO_4^{3-} + 2OH^- \qquad \textbf{\textit{Equation 1}}$$

The state of equilibrium varies to a great extent with pH. At the average pH of normal resting (unstimulated) saliva, there is little to no occurrence of demineralization because the salivary fluid is supersaturated with respect to Ca^{2+} and PO_4^{3-} ions. At the acid pH, the solubility of HA increases, which promotes the enamel demineralization. On the contrary, if the dental microenvironment is supersaturated with Ca^{2+} and PO_4^{3-} ions after the pH increases, a partial remineralization of HA occurs on the dental enamel surface (7).

Despite the fact that the dental enamel mainly constitutes of HA, some other metal ions, such as Na^+, Mg^{2+}, and K^+, have the ability to replace some Ca^{2+} ions and disturb the crystal lattice of HA, whereas F^- ions have the capacity to replace OH^- ions in the HA lattice. As a result, these ion substitutions in mineral crystal lattice of enamel and dentin render the tooth surface much more acid soluble. In spite of this, the incorporation of F^- into HA improves and strengthens its crystal structure and renders the dental enamel more resistant against acid-induced dissolution (8).

1.1.2 Salivary Fluid

Saliva is a watery mixture of fluids excreted by salivary glands into the oral cavity. In humans, this exocrine secretion consists approximately 99 % of water and contains wide variety of compounds, such as electrolytes (sodium, potassium, calcium, chloride, magnesium, bicarbonate, phosphate, iodine), mucosal glycoproteins (mucins), enzymes (α-amylase, lipase, lysozyme, lactoperoxidase, lactoferrin, immunoglobulin A etc.), traces of albumin, desquamated epithelial and blood cells, bacteria, urea, and food detritus (9). When secreted it is isotonic with respect to plasma, but later becomes hypotonic as it travels through the network of ducts.

A healthy person produces from 1 to 1.5 L of salivary fluid per day. The normal salivary flow ranges from 0.25 mL/min to 0.35 mL/min, and can be increased dramatically to reach 1–3 mL/min (9). Its composition varies to a great extent among individuals (9).

Salivary fluid plays an essential role in protecting and maintaining the oral health. It serves a lubricative function, moisturizes the food, dilutes and cleans the content from oral cavity. The enzymes present in saliva (mostly α-amylase) are responsible for the initial processing of dietary starches and fat. They also disintegrate food residue within dental crevices, thus safeguarding dental enamel from bacterial decay. Furthermore, the mucins in salivary fluid, as constituents of seromucosal layer called mucus, lubricate oral tissue surfaces and

protects them against dehydration as well as various irritating agents. In addition, mucins have the capacity to influence the bacterial and fungal colonization by modulating microorganism adhesion onto oral tissue surfaces (9).

One of the most important roles of salivary fluid is to act as a buffer system to protect the oral cavity, namely by maintaining a natural pH. In particular, saliva inhibits potentially pathogenic microorganisms by impeding their optimal growth conditions, while it also inhibits the tooth demineralization by neutralizing and eliminating the acids produced by oral microorganisms. The most essential buffer in saliva is carbonic acid-bicarbonate system, followed by urea and sialin (a salivary protein) buffers. In addition, the presence of calcium and phosphate ions in the salivary fluid facilitates remineralization of both carious and non-carious tooth (9).

1.1.3 Dental Pellicle

The dental pellicle or the acquired enamel pellicle is a thin organic biofilm on the surface of dental enamel formed by the adsorption of specific salivary components, namely glycoproteins, that offers protection against continuous calcium phosphate erosion, as a result of acids produced my acidogenic microorganisms after consuming carbohydrates. It forms swiftly after the teeth are washed or after chewing and serves as a lubricating agent by reducing friction between teeth and the other oral surfaces. Additionally, the pellicle layer acts as a selective permeability barrier for ionic species by impeding enamel dissolution when exposed to acidic conditions. The distribution of Ca^{2+} and PO_4^{3-} ions from the enamel to microenvironment is thus slowed and the penetration of acids through the pellicle toward the enamel is stalled. The pellicle also inhibits the adsorption of cariogenic microorganisms onto dental surface and thus protects the teeth (10).

After carbohydrates are consumed, oral bacteria metabolize sugars producing lactic acid, which decreases pH of saliva and pellicle (*Streptococcus mutans* ceases to metabolize sugars at pH values bellow 4.2 (11)), and makes these fluids undersaturated with Ca^{2+} and PO_4^{3-} ions with respect to enamel ($4.5 < pH < 5.5$), consequently increasing the HA solubility; process is depicted in *Figure 3*. As a result of this shift favoring demineralization, the loss of calcium and phosphate ions from the enamel crystal subsurface occurs until the equilibrium between de- and remineralization is restored. This happens with the assistance of buffering capacity of saliva complemented with outward diffusion of acids from dental

pellicle, which promotes the increase in biofilm pH within a few minutes. When the pH becomes greater than 5.5, the supersaturation of the oral fluids with dissolved HA is restored, resulting in remineralization of dental enamel (5).

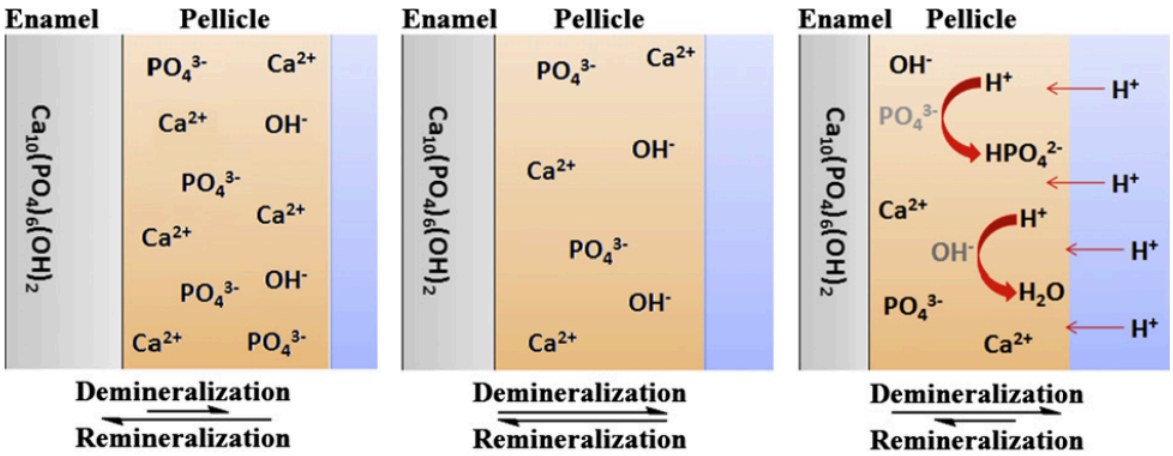

***Figure 3**: Chemical conditions in oral cavity associated with dental enamel remineralization (left), equilibrium between enamel production and demineralization (middle), and enamel demineralization due to the acidic attack (right) (12).*

1.1.4 Oral Mucosa

The oral mucosa is a moist mucosal membrane covering the oral cavity. It serves a protective function against compressive and shearing forces, and acts as a barrier for microorganisms, toxins and antigens while providing a first line of immunological defense (both humoral and cell-mediated). It is rich in minor glands that offer lubrication, buffering and secrete certain antibodies. Its viscoelastic properties assist in water and electrolyte retaining. The oral mucosa is well-innervated, detecting stimuli by proprioception, nociception, gustatory perception, and a sense of touch (4).

The oral mucosa is comprised of two distinctive layers depicted in *Figure 4*. The outer layer is a stratified squamous epithelium containing keratin; beneath the epithelium is a connective tissue called the lamia propria. The boundary between them is often indistinct. The keratinized epithelium constitutes of four layers: ① the base layer (*stratum basale*), ② the prickle layer (*stratum spinosum*), ③ the granular layer (*stratum granulosum*), and ④ the keratinized layer (*stratum corneum*).

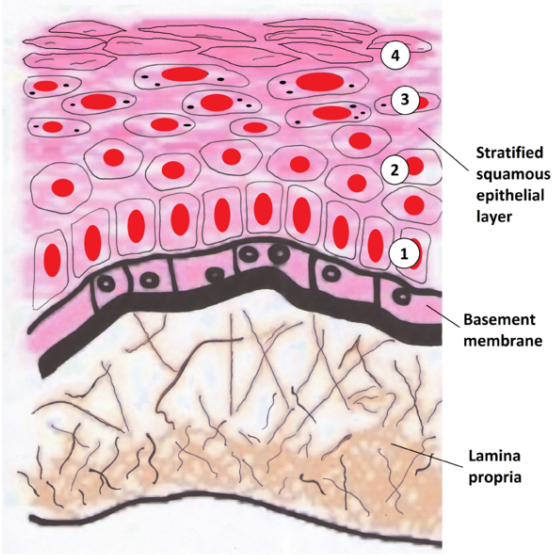

***Figure 4**: The structure of oral mucosa comprised of two distinctive layers: the surface stratified squamous epithelium and the deeper lying lamina propria (13).*

The oral mucosa occupies approximately 170 cm^2 total surface area of oral cavity with the teeth, keratinized epithelium, and non-keratinized epithelium encompassing 20 %, 50 %, and 30 %, respectively (14).

1.2 Prevalent Oral Diseases and Conditions

The most prevalent oral diseases and conditions nowadays are dental caries, periodontitis, tooth loss, oral cancer, oral infectious disease, trauma from injuries, and hereditary lesions. World Health Organization (WHO) reports that globally, about 30 % of people aged 65–74 have no natural teeth (15). The major cause of dental loss is dental caries and periodontal disease. The most common risk factors for oral diseases involve an unhealthy diet, tobacco use, and harmful alcohol consumption.

Worldwide, 60–90 % of school children and nearly 100 % of adults have tooth decay, which is the most widespread non-communicable disease (NCD) globally (2, 15). Tooth decay, also referred to as dental caries or cavities, occurs when oral bacteria adhered onto dental pellicle or the plain tooth surface develop into biofilm, known as the dental plaque (4). The most prominent bacteria responsible for onset and development of dental caries are *Streptococcus mutans* and *Streptococcus sobrinus* and *Lactobacilli*. Frequent dietary sugar intake is followed by fermentation of carbohydrates and production of lactic acid,

which causes a localized demineralization of dental enamel. If the site is not remineralized through saliva's buffering capabilities or effect of F^-, the damage can become irreversible and lead to tooth decay. As a result, a professional treatment is required to stop and prevent any further unfavorable processes.

Severe periodontitis, which may lead to tooth loss, is found in 15–20 % of middle-aged (35–44 years old) adults (15). It is more prevalent in smokers, diabetics, people living with HIV/AIDS and in those who use certain medication. Periodontitis is an inflammation of soft and hard structures that support teeth. It develops from gingivitis, which can be characterized by red, swollen, and potentially bleeding gums induced by bacteria present in dental plaque. In its most severe form, the gums can separate from the tooth, alveolar bone can be impaired, and teeth may loosen or fall out. A good oral hygiene, a professional teeth cleaning, a surgical or non-surgical plaque removal by dental professional is essential in its treatment. Moreover, most treatments include administration of antimicrobials solutions (e.g. chlorhexidine) or antibiotics, such as metronidazole, minocycline, and doxycycline (16).

1.3 Novel Drug Delivery Systems

For a long time, the treatment of acute and chronic diseases has been accomplished by administering conventional pharmaceutical formulations, such as tablets, pills, capsules, powders, syrups, syringes, pastes, creams, gels, ointments, liquids, aerosols. These delivery systems for active pharmaceutical ingredients (APIs) are present and used globally even nowadays. This type of drug delivery systems (DDS) often provide only instant release of API and exert systemic effects that closely correlate with the onset of adverse effects. For that reason, novel DDSs have been intensively investigated in recent years. Several technological advancements assure local, site-specific controlled drug delivery, which avoids first-pass metabolism (17).

The advancements in nanomedicine in recent years have brought great focus to nanotechnological developments in the field of DDSs, which could be employed for the treatment of oral conditions. Various nanodelivery systems, including nanoparticles, either nanospheres or nanocapsules, liposomes, dendrimers, nanocrystals and nanofibers, have been investigated for application in dentistry (18). These systems are generally in form of low

viscous aqueous dispersions, which ensures a uniform distribution of the formulation in the oral cavity, or can be integrated in semisolid dosage forms (18).

Polymeric nanoparticles (NPs) are nanospheres consisting of polymer matrix of interwoven polymer chains. Various therapeutic agents can be incorporated in their structure. Liposomes, in comparison to polymeric NPs *(Figure 5*), are self-assembled lipid vesicles consisting of amphiphilic molecules, namely phospholipids, that have the capacity to encapsulate molecules either in their hydrophilic core or in their bilayered membrane or in both. The ideal nanodelivery systems are biodegradable, biocompatible, non-toxic, and offer bioadhesive properties (19).

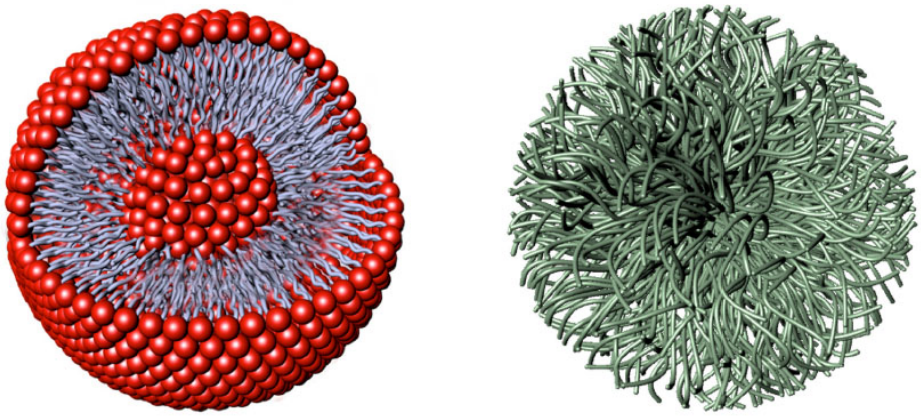

***Figure 5**: Schematic representation of liposome (left) and polymeric NP (right) (20).*

Polymer NPs and liposomes can provide sustained drug release or the drug release can be triggered in response to a specific environmental stimulus (21). They can adhere onto specific oral surfaces, such as teeth and oral mucosa, and thus improve drug availability. Furthermore, they can protect the incorporated drug from various environmental adverse effects (e.g., interactions with saliva and oral microorganisms) (22).

1.4 Compounds Used in the Research Work

1.4.1 Chitosan

Chitosan is a linear cationic polymer derived from chitin (*N*-acetyl-β-D-glucosamine) and produced from crab or shrimp shells and fungal mycelia. It consists of deacetylated D-

glucosamine and acetylated *N*-acetyl-D-glucosamine. It is the second most abundant natural polysaccharide after cellulose. Its structure is depicted in *Figure 6*. It is characterized as a weak base and is insoluble in water and different organic solvents. Nevertheless, it is soluble in dilute aqueous acidic solutions (pH < 6.5) and concentrated acids (23). When exposed to alkaline solutions or polyanions, it precipitates, whereas it forms gel at lower pH, if concentration of the polymer is high enough. It is inexpensive, bioadhesive, biodegradable, biocompatible, non-toxic for mammals and, at the same time, shows antimicrobial activity against various groups of microorganisms (24). Besides that, it has been reported that it can act as an antitumor agent and possess antioxidant properties (25). For that and many other reasons, it is commonly used in pharmaceutical and many other biomedical applications.

Chitosan was used as a polymer in preparation of chitosan NPs in the present thesis.

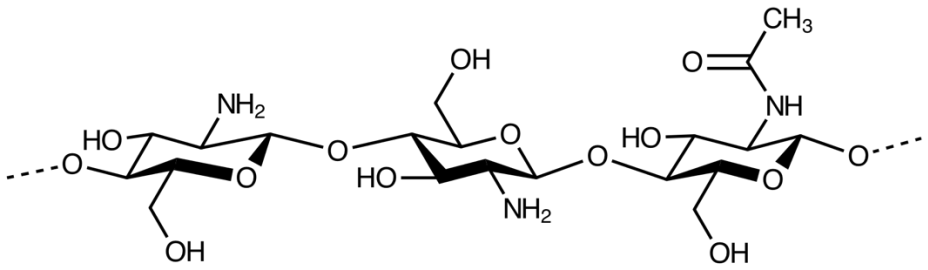

***Figure 6**: Chemical structure of chitosan.*

1.4.2 Fluorescein Isothiocyanate

Fluorescein isothiocyanate (FITC) is a derivative of fluorescein with formula $C_{21}H_{11}NO_5S$, and IUPAC name 2-(6-Hydroxy-3-oxo-3H-xanthen-9-yl)-5-isothiocyanatobenzoic acid shown in *Figure 7*. It is commonly used as a fluorescent label. In FITC, the isothiocyanate group (–N=C=S) is attached to the para- position of benzene ring. This derivatization enables reactions with nucleophiles including sulfhydryl and amine groups of proteins. FITC has excitation maximum and emission minimum wavelengths of 495 nm and 519 nm, respectively. It is sensitive to pH changes, photosensitive, and shows relatively high rate of photobleaching (26). Photobleaching is a phenomenon commonly referred to as fading which occurs when a fluorophore permanently loses the ability to fluoresce due to irreversible photochemical damage (27).

In this thesis, FITC was utilized as fluorescent label for chitosan NPs.

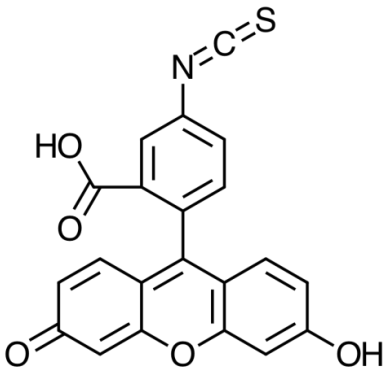

***Figure 7**: Chemical structure of fluorescein isothiocyanate.*

1.4.3 Tripolyphosphate

Sodium tripolyphosphate (TPP) is the sodium salt of the polyphosphate penta-anion with formula $Na_5P_3O_{10}$, depicted in *Figure 8*. The polyanionic moiety is penta-ionic chain $[O_3POP(O)_2OPO_3]^{5-}$, which tends to bind strongly to cations. In pharmaceutical and bio-medical applications, TPP is the most popular polyanion because it shows non-toxic properties and quick gelling ability with positively charged entities, such as chitosan used in this research work (28). It is often used as a cross-linking agent in polysaccharide-based DDSs due to its ability to mediate the formation of inter- and intramolecular cross-links with oppositely charged functional groups of polysaccharides.

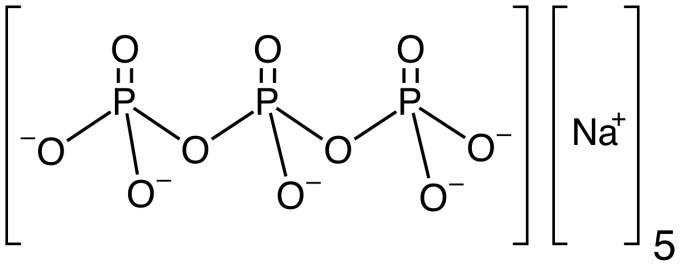

***Figure 8**: Chemical structure of sodium tripolyphosphate.*

1.4.4 Sodium Fluoride

Sodium fluoride is an ionic compound with chemical formula NaF. When dissolved, it gives Na^+ and F^- ions. It is in a form of white odorless powder. It is listed in WHO Model List of Essential Medicines, which provides a comprehensive list of minimum medicines needed for a basic health-care system (29).

Fluoride is most commonly used in a form of a sodium fluoride and is one of the main ingredients of almost all toothpastes commercially available today. It is considered to be the most effective anti-caries agent with potent anti-bacterial effect. In detail, fluoride ion is capable of replacing hydroxyl (OH^-) ion in crystalline structure of HA, thus forming fluoroapatite (FA), a substituted crystal. The incorporation of fluoride into tooth enamel is represented in *Equation 2*.

$$\underset{\textit{Hydroxyapatite}}{Ca_{10}(PO_4)_6(OH)_2} + 2F^- \rightleftharpoons \underset{\textit{Fluoroapatite}}{Ca_{10}(PO_4)_6F_2} + 2OH^- \qquad \textbf{\textit{Equation 2}}$$

Furthermore, one of the benefits of brushing teeth with tooth paste containing fluoride is the formation of calcium fluoride (CaF_2) in dental pellicle and on the surface of the enamel. When the pH in oral cavity is lowered, the accumulated fluoride and calcium ions get released from dental pellicle and the former diffuse along with acid from pellicle into the enamel pores, where they promote the formation of resistant FA and strengthen the tooth surface. In comparison to HA, the inclusion of FA increases the resistance of enamel to acidic attack because it decreases the critical pH of dissolution of the enamel (FA's critical pH is 4.5, whereas HA's critical pH equals 5.5) (30). In addition, fluoride also promotes remineralization and hinders demineralization of tooth enamel in environment with pH between 4.5–5.5. To elaborate, after the acid-induced enamel dissolution concludes, the pH in oral cavity starts rising back towards natural level (pH 7.0) and, in the process, reaches FA's critical pH quicker than HA's critical pH. Hence, the shorter demineralization period as a result of F^- ions embedded in crystal lattice of tooth enamel (30).

Apart from the enamel protecting abilities, fluoride is believed to have anti-bacterial effect. In acidic environment of oral cavity, fluoride can be present also in form of hydrogen fluoride (HF). Due to being undissociated weak acid, HF can penetrate bacterial cell membrane and enter its cytoplasm, where it dissociates to H^+ and F^- ions. Both ions interact with cellular components: F^- ions negatively impact certain fluoride-sensitive enzymes, whereas protons exert great stress to various cellular constituents, especially enzymes responsible for cell growth (30), by lowering intracellular pH. Moreover, the cellular excess proton-coping mechanisms are suppressed by F^- ions.

In the present thesis, NaF was used as an API for incorporation into chitosan NPs.

1.5 Nanoparticles for Dental Application

In the present thesis, polysaccharide-based NPs were investigated. Chitosan was employed as one of the most investigated polysaccharides due to its biocompatibility, biodegradability, bioadhesive properties and nontoxicity. Interestingly, chitosan NPs have already been reported to have both anti-inflammatory and antibacterial effect (31). Due to their small size, NPs in general are believed to have a great benefit in accessing the areas that are unreachable to other drug delivery systems (32).

Ideal NPs for drug delivery should have a low PDI, leading to their uniform attributes, such as drug release rate and drug targeting ability (33, 34). The particle size has the greatest effect on the biodistribution of NPs and is also directly contingent on the target site of the NPs (34). For dental applications, the particle size range of 100–500 nm could be beneficial as such structures resemble micelle-like structures normally present in saliva (35, 36). Evidence shows that the sizes of the NPs depend on the order of addition of cross-linker during formation process. Hence, the sizes of NPs increase proportionally with concentration of cross-linking agent due to the increase of collisions between polymer and cross-linker (37). Furthermore, a faster NP formation is reflected in less homogeneous particles size distribution (38). Ideally, NPs administered into oral cavity should not have any adverse effects, be biocompatible, and stable in order for the API to fully reach and effect its target site.

Chitosan NPs described in this thesis were prepared by ionotropic gelation method. The process of ionotropic gelation happens when positively charged polymer interacts with negatively charged (poly)anion. In our case, the formation of NPs through ionic cross-linking happened between positively charged chitosan and negatively charged TPP.

1.6 Nanoparticle Characterization Methods Used in the Research Work

1.6.1 Dynamic Light Scattering

Dynamic light scattering (DLS) is a non-invasive technique employed to measure size of particles and molecules in colloidal dispersions, with size of dispersed phase in the range from ~0.1 nm to ~10 μm. The technique detects and measures random particle movement called Brownian motion and then employs the Stokes-Einstein equation to determine particle size and size distribution (39).

Brownian motion occurs when particles suspended in liquid or gas randomly move as a result of collisions with fast-moving molecules of the quiescent fluid. At certain temperature, large colloidal particles move slower compared to small particles. The diffusion velocity of a particle undergoing Brownian motion is described by Stokes-Einstein equation (*Equation 3*).

$$D = \frac{k_B T}{3\pi\eta R}$$

D ... diffusion coefficient
k_B ... Boltzmann constant
T ... temperature
η ... viscosity of dispersion medium
R ... hydrodynamic diameter

Equation 3

The diameter that DLS measures is called the hydrodynamic diameter. It closely correlates to the velocity of a particle diffusing in the fluid. To be more specific, the diameter procured by DLS equals that of a sphere that is larger than a particle core due to the structures adsorbed onto the particle surface, but has the identical translational diffusion coefficient as the measured particle (40).

A DLS system operates by illuminating particles in the sample by laser light. Light scattered by the particles is collected by a detector that converts it into electrical pulses which are sent into a digital correlator that yields autocorrelation function. From that function, the particle sizes are calculated (39).

In addition, DLS systems have the capacity to record the intensity of light scattering as the measurement of derived count rate, which closely correlates to the number of photons per second arriving at the detector. This is often referred to as counts per second or kilo counts per second (kcps) (41).

Zetasizer, the system used for measurements in the research, has a very large dynamic range when it comes to scattering detection. The attenuator is used when the system detects the light intensity too high for the sensitive photon detector. In that case, the system blocks some of the signal but only measures a tiny amount of it with the use of an attenuator. Correlation between attenuator index and percentage of light transmitted is shown in *Table I* (41).

***Table I**: Correlation between attenuator index and light transmission levels.*

Attenuator Index	Transmission (% Nominal)	Attenuator Index	Transmission (% Nominal)
0	0	6	0.3
1	0.0003	7	1
2	0.003	8	3
3	0.01	9	10
4	0.03	10	30
5	0.1	11	100

In short, the higher the attenuator index, the less particle scattering has been detected by a photon detector, and vice versa. In other words, particle concentration in sample can also be closely correlated to the attenuator index: the higher it is, the lower the particle concentration and/or the smaller particles, and the other way around.

1.6.2 Fluorescence Spectroscopy

Fluorescence spectroscopy is a method for detecting and analyzing the analyte concentration in sample based on its fluorescent characteristics (42).

Fluorescence is a phenomenon that occurs when an atom or a molecule absorbs energy (a photon), usually light in ultraviolet spectra, and transitions an orbital electron to an excited singlet state of higher energy. In order of nano- and picoseconds after the excitation, an atom or a molecule reverts to ground electronic state while emitting a photon of a longer wavelength, typically but not necessarily in the visible region of the spectrum (43).

The analytes used in fluorescence spectroscopy must be water-, ethanol-, or hexane-soluble. They need to have the ability to absorb UV or visible light and emit light in visible or near infra-red spectra. Since only a relatively small number of substances are able to fluoresce, some non-fluorescent compounds can be made fluorescent by labeling them with a fluorescent dye, such as fluorescein used in present thesis (42).

2 OBJECTIVES

The overall aim of this master's thesis is to develop physically stable polymer NPs loaded with fluoride as an API. Chitosan will be used for NP preparation due to its bioadhesive properties, biodegradability, biocompatibility and non-toxicity. The polymer NPs will be prepared by a self-assembling technique called ionotropic gelation.

The sub-aims of this thesis are to:

1. Prepare and characterize fluoride-loaded NPs and fluorescently-labeled fluoride-loaded NPs in order to use fluorescence as a quantitative method for determination of the adsorption of NPs onto HA (see the sub-aim number 4).
2. Evaluate gel-filtration as a separation method and investigate its efficacy in separation of fluoride-loaded nanoparticulate structures from free molecules (i.e. unentrapped fluoride, polymer chains, unbound fluorescent dye).
3. Perform interaction studies with artificial saliva in order to discover whether the presence of salivary components affects the structure and behavior of fluoride-loaded NPs.
4. Perform interaction studies of NPs with HA to investigate to which extent the fluoride-loaded NPs adsorb onto HA.
5. Perform interaction studies of NPs with mucins to investigate possible mucoadhesivity of NPs.

3 MATERIALS AND METHODS

3.1 Materials

The following materials and substances were used in this thesis: polymer used was chitosan-HCl (Protasan™ UP CL 213, NovaMatrix®, Norway), sodium fluoride was used as an API (Sigma-Aldrich®, Germany), sodium tripolyphosphate pentabasic (Sigma-Aldrich®, Germany) was employed as a cross-linker, and fluorescein isothiocyanate isomer I (Sigma-Aldrich®, Germany) was used as a chitosan-labeling agent. Fluoride-labeled chitosan used in this research was prepared by Sara Pistone. NPs were prepared using water purified and filtered by a Milli-Q® Integral Water Purification System (Merck KGaA, Germany).
To test adsorption of gel-filtered FITC-labeled fluoride-loaded chitosan NPs onto HA, a hydroxyapatite powder (nanoXIM•HAp403 10 μm spray-dried powder, Fluidinova, Portugal) was used. To test interactions of NPs with mucins, mucins from porcine stomach, type II (Sigma-Aldrich®, Germany), were employed.

3.2 Preparation of Fluoride-loaded Chitosan Nanoparticles

To begin with, stock solutions of chitosan (0.1167 % (w/w)), NaF (1.0000 % (w/w)) and TPP (0.0875 % (w/w)) were prepared using the water purified and filtered by Milli-Q system (Milli-Q water). All solutions were left at a room temperature overnight covered by parafilm, except the stock solution of TPP which was stored in a refrigerator. It should be noted that the polymer solution was stirred overnight so the chitosan could fully dissolve. When chitosan used was FITC-labeled, the beaker was fully covered with aluminum foil due to FITC' photosensitivity.
Next, 45 g of chitosan stock solution was filtered using 0.8 μm sterile syringe filter (Millex® AA syringe filter unit, ethylene oxide sterilized) in the 100 mL vial rinsed with Milli-Q water; 15 g of TPP stock solution and 15 g of NaF stock solution were both filtered using 0.22 μm sterile syringe filters (VWR®, syringe filter with acrylic housing, sterilized) each in its own previously rinsed 20 mL vial.
A Watson-Marlov 520S peristaltic pump shown in the *Figure 9* was used to introduce NaF and TPP solutions into the chitosan solution. Firstly, the appropriate tubing was fit inside

the pump and then rinsed by pumping 30 mL Milli-Q water through it at high speed (90–110 rpm). The external edges of the tubing were rinsed with Milli-Q water as well.

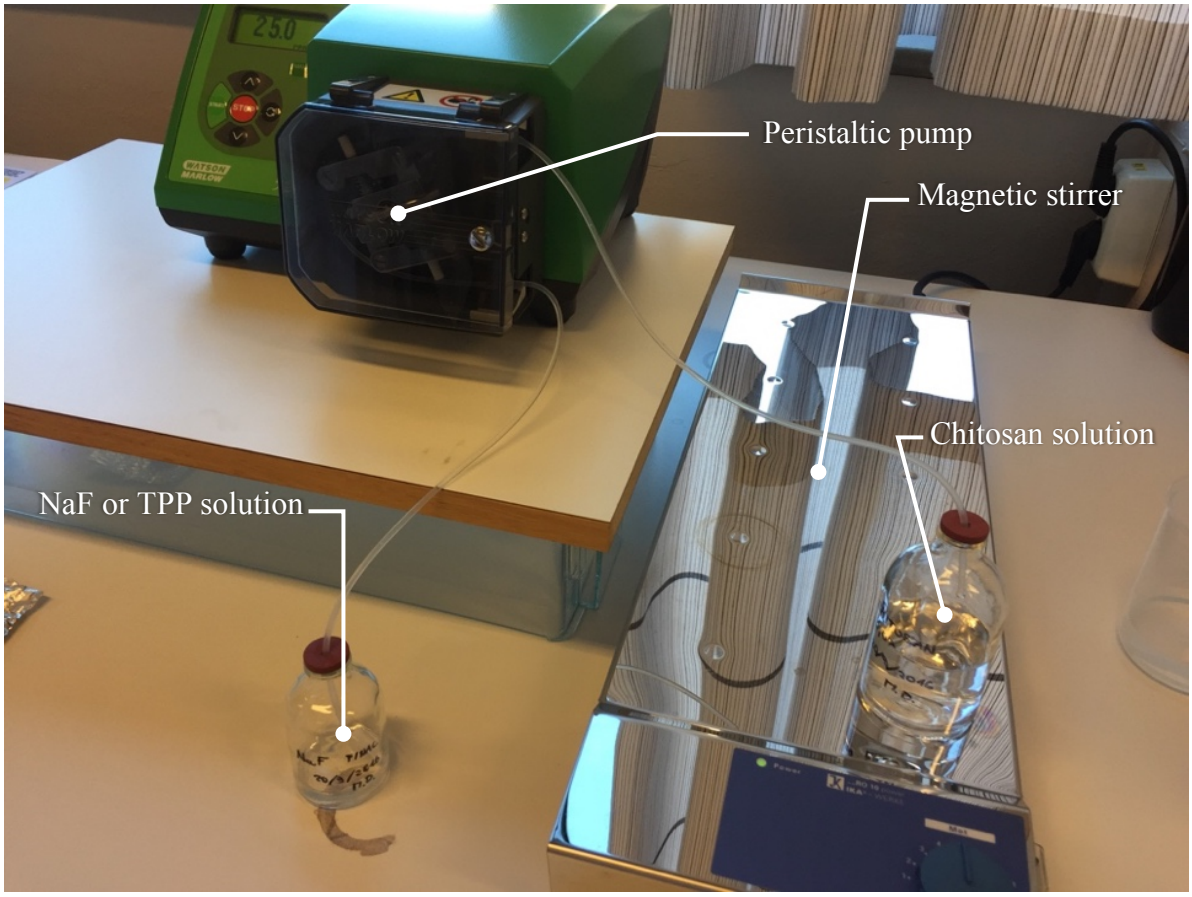

***Figure 9**: Setup for NP preparation with the peristaltic pump.*

Secondly, the tubing was rinsed with 20 mL NaF solution at 110 rpm. A magnet (length 2 cm) was rinsed with Milli-Q water, put in the vial with chitosan solution and placed on the magnetic stirrer at stirring speed level 5. One end of the tubing (the one from which the drops of polymer solution were coming out) was installed into the vial with chitosan solution in order to let the NaF solution drop in the middle of the swirl formed in the chitosan solution while mixing. The vial with chitosan solution was closed with the stopper pierced with the tubing. The other end of the tubing was submerged in the NaF solution so the tubing reached the bottom of the vial. This vial was also closed with the stopper that came with the tubing. Afterwards, the pump was started at 25 rpm. When the first drop of NaF solution fell into the chitosan solution, the chronometer was started (10 min total stirring time). The time when the last drop fell was noted in order to control that the pump was

operating well. Chitosan solution was stirred until the alarm went off. Then, the vial was closed with the rinsed stopper.

Lastly, the tubing was rinsed with 20 mL of the TPP solution at 110 rpm. The vial with chitosan-NaF mixture was placed on magnetic stirrer at stirring speed level 5. TPP solution was then pumped to the mixture at 25 rpm similarly as described with NaF solution. The dispersion was mixed for 10 min. In the end, the vial containing sample was closed with rinsed stopper and the tubing was rinsed by pumping 20 mL Milli-Q water through it at 110 rpm.

This procedure yielded fluoride-loaded chitosan NP dispersion with 0.07 % (w/w) chitosan. TPP-to-chitosan ratio was 20:80 (w:w) and it contained 0.2 % (w/w) NaF.

All samples were kept overnight at room temperature. During the sample preparation, the same size of magnets, vials, and other equipment were used because shear forces created during preparation process could have influenced the resulting NP size.

3.3 Preparation of FITC-labeled Chitosan

In scope of the research, the chitosan was not labeled with FITC on our own, but prepared according to the following method.

1 g of chitosan was dissolved in 200 mL of Milli-Q water and then 200 mL of methanol was added. 100 mg of FITC was dissolved in 100 mL of methanol and added to the chitosan solution. The chitosan–FITC solution was mixed for 3 h in the Erlenmeyer flask wrapped in an aluminum foil. Next, the chitosan was precipitated by adding a solution of NaOH, 0.1 M, until pH 7 was reached. The precipitated chitosan was centrifuged for 10 min at 4400 rpm. The supernatant was discarded.

The precipitate was rinsed 4 times (or until the supernatant was transparent) as follows: a solution of ethanol:water (7:3) was added in the centrifuge tube with the pellet, the pellet was suspended and dispersion was centrifuged again for 10 min at 4400 rpm. After discarding the clear supernatant for the last time, the chitosan–FITC pellet was dissolved in the minimum amount possible of HCl, 0.6 M.

In the next step, the chitosan–FITC solution was dialyzed against Milli-Q water. For the dialysis, 2 cylinders were used (each 1 L). All equipment was wrapped in the aluminum foil and kept in the refrigerator. The water for the dialysis was changed twice per day until no fluorescence was detected in the water. A sample of the water used for dialysis was

measured against Milli-Q water using Victor^3 1420 Multilabel Counter (PerkinElmer, the United States of America).

The dialyzed chitosan–FITC solution was freeze-dried and stored in the refrigerator protected from light.

3.4 Preparation of Fluorescently-labeled Fluoride-loaded Nanoparticles

The process of preparing fluorescently-labeled fluoride-loaded NPs was exactly the same as described in *Chapter 3.2* with the following exception: 5 % of chitosan used for preparation of chitosan stock solution was FITC-labeled, whereas other 95 % was unlabeled chitosan.

3.5 Characterization of Nanoparticles

3.5.1 Average Particle Size and Particle Size Distribution

The cuvette and its lid were rinsed with Milly-Q water to remove potential dust and other contaminants. The cuvette was then filled with 1 mL of sample and carefully inspected for any visible particles or air bubbles. The outer sides of the cuvette were cleaned with lens cleaning paper before the cuvette was placed into the instrument's measuring cell. All measuring parameters were set (*Table II*) and finally the measurement was initialized using computer software.

***Table II**: Parameters used in determination of particle size and PDI.*

Instrument:	Zetasizer Nano ZS, Malvern Instruments Ltd
Sample Container:	Disposable polystyrene cuvette (10 × 10 × 45 mm), Sarstedt AG & Co., Nümbrecht, Germany
Sample volume:	1 mL
Approximation:	Mark-Houwink-parameter
Measuring temperature:	25 °C
Equilibration time:	300 s

Measuring angle:	173°
Duration (each measurement):	automatic
Number of measurements:	3
Attenuator:	automatic

3.5.1 pH Measurements

The pH of NP samples was measured at room temperature with a 744 Metrohm pH Meter (Metrohm, Switzerland) calibrated using two buffers between pH 4 and 7. For the measurements of the pH to be valid the deviation had to be within ± 3 %.

3.5.2 Visual Inspection

Visual inspection was performed for all the NP samples. Samples were observed against a light and in front of a black screen. Presence of any larger aggregates, flocculates or sediment was also noted.

3.5.3 Quantification of Nanoparticles by Fluorescence Spectroscopy

Firstly, blank solutions were prepared in Eppendorf tubes (from the samples that did not contain HA powder or mucins): for each point of the calibration curve, a solution of total volume of 1 mL was prepared (100 % = 1 mL blank, 80 % = 0.8 mL of blank + 0.2 mL of the same medium as in GF NP dispersion, 60 % = 0.6 mL of blank + 0.4 mL of medium, etc.).

Secondly, from each supernatant obtained as described in *Chapter 3.8* and *3.9*, 100 µL were transferred into a well of a white 96-well flat-bottomed microtiter plate (Nunc, Denmark). This step was repeated 2 more times to obtain 3 parallel wells filled with samples. From each blank solution, 3-times 100 µL were transferred to the same plate as well.

To measure fluorescence a Victor^3 1420 Multilabel Counter (PerkinElmer, the United States of America) was employed. The system settings were configured as shown in *Table III*. The measurements were performed at λ_{ex} 485 nm, λ_{em} 535 nm.

***Table III**: Settings used for fluorescence measurements with Victor³ 1420 Multilabel Counter.*

Name of the plate type:	Generic 8 × 12 size plate
Number of repetitions:	1
Delay between repetitions:	0 s
Measurement height:	Default
Shaking duration:	3 s
Shaking speed:	Fast
Shaking diameter:	0.10 mm
Shaking type:	Linear
Repeated operation:	Yes
Label technology:	Prompt fluorometry
CW-lamp filter name:	F485
CW-filter slot:	A5
Emission filter name:	F535
Emission filter slot:	A5
Measurement time:	0.1 s
Emission aperture:	Normal
CW-lamp energy:	500
2nd measurement CW-lamp energy:	500
CW-lamp control:	Stabilized energy

3.6 Purification of Nanoparticles by Gel-filtration

In the process of gel filtration PD-10 desalting columns (GE Healthcare Bio-Sciences AB, Sweden) containing 8.3 mL of Sephadex™ G-25 medium were used. The column setup is shown in *Figure 10.* The gel-filtration was performed according to the gravity protocol.
At first, PD-10 desalting column was prepared by removing the top cap and pouring off the column storage solution. The sealed end of the column was cut at notch.

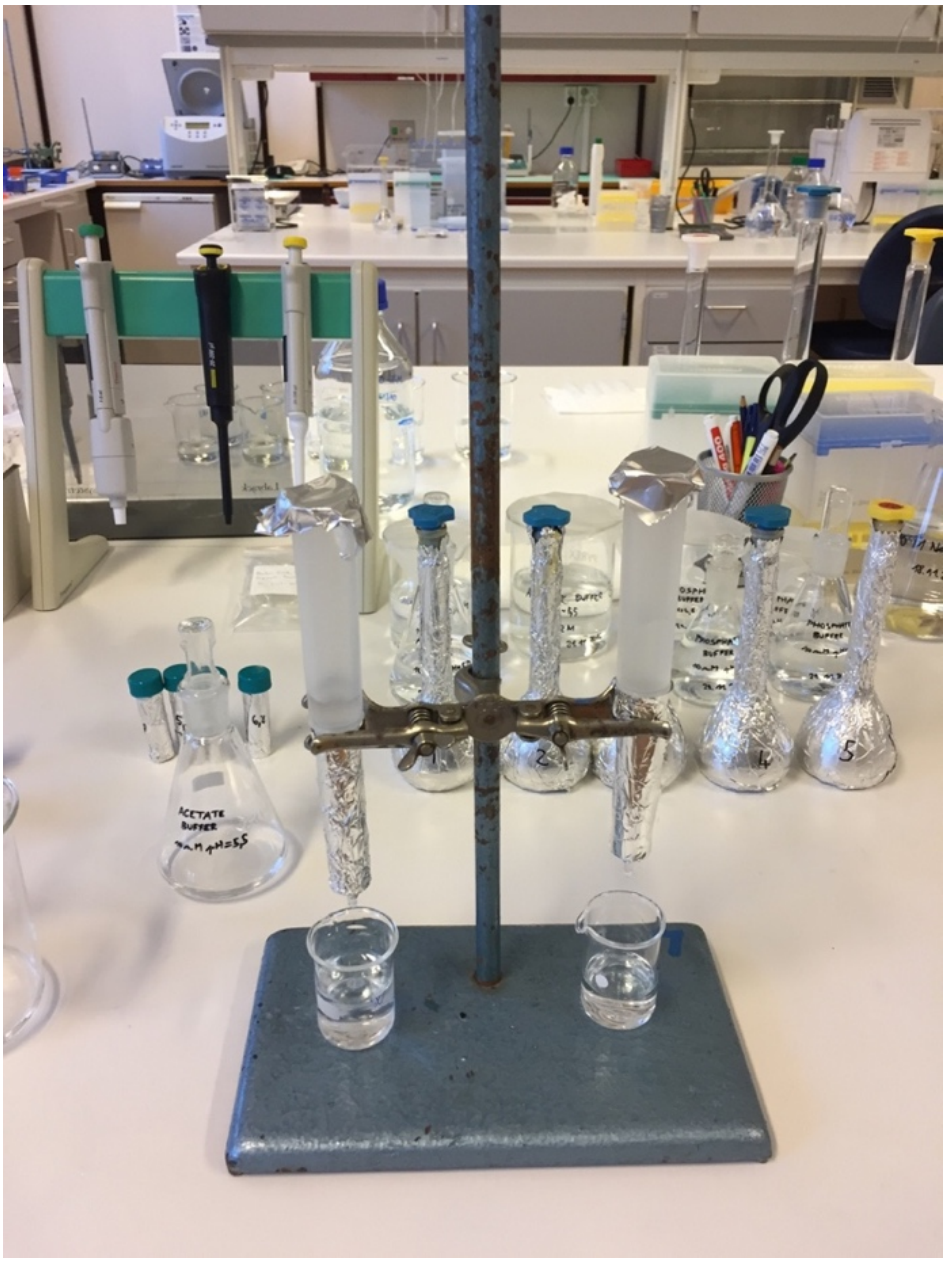

***Figure 10**: Gel-filtration setup.*

Next, the column was filled with 25 mL of equilibration buffer (10 mM acetate buffer pH 5.5 or 10 mM phosphate buffer pH 6.8). The flow-through was discarded in 10 mL beakers. In the following step, 2.5 mL of sample was added to the column. After the sample had entered the packed bed completely, all the collected flow-through was discarded. Finally, the sample was eluted with 3.5 mL buffer and the eluate collected in a 5-mL container.

Throughout the process, aluminum foil was used to cover the top of the columns during elution to prevent any possible contaminations. If FITC-labeled NPs were purified, the whole column was covered in aluminum foil to protect the sample from the light.

3.7 Interaction Study of Nanoparticles with Salivary Electrolytes

For the purpose of *in vitro* interaction studies of NPs with an artificial saliva the SAGF medium was chosen with its composition as presented in *Table IV* (44).

***Table IV**: Composition of the SAGF medium with concentrations of compounds in the final solution.*

Compound	Concentration [mg/L]	Compound	Concentration [mg/L]
NaCl	125.6	$Na_2SO_4 \times 10H_2O$	763.2
KCl	963.9	NH_4Cl	178.0
KSCN	189.2	$CaCl_2 \times 2H_2O$	227.8
KH_2PO_4	654.5	$NaHCO_3$	630.8
Urea	200.0		

Each solution was individually prepared using the compounds stated in the *Table IV* using Milli-Q water as a solvent. All solutions were stirred individually for 20 min on a magnetic stirrer at a room temperature and thereafter mixed together and stirred for additional 20 min on a magnetic stirrer. Before the interaction experiments were performed, the pH value of the SAGF medium was adjusted to 6.8.

For the interaction experiments, 2.5 mL of artificial saliva was mixed with 0.5 mL of NP sample in a centrifuge tube and spun the sample at 20 rpm for 5 min at 35 °C using test-tube rotator (Model LD79, Labinco BV, the Netherlands). As samples, both gel-filtered (GF) and non-gel-filtered (NGF) NP formulations were used. A total number of 2 parallels for each combination was prepared.

For evaluation of interaction of NPs with salivary electrolytes in order to explore effects on NP aggregation and stability, the measuring temperature was set to 37 °C, whereas the number of measurements was set to 100. The Zetasizer ran for 2 h. During the experiment average particle sizes and particle size distributions were recorded every 2 min. The first measurement was recorded 5 min after mixing in order to achieve temperature equilibration of the sample.

3.8 Adsorption of Nanoparticles onto Hydroxyapatite Powder

GF FITC-labeled fluoride-loaded chitosan NPs were used in the adsorption studies onto HA powder.

Firstly, 6 test tubes with stoppers containing 20 mg, 40 mg, 80 mg, 10 mg, 150 mg and 200 mg of HA powder were prepared. 1.0 mL of medium (10 mM acetate buffer pH 5.5 or 10 mM phosphate buffer pH 6.8 – depending on the solvent used for gel-filtration of NPs) was added. Moreover, 2 extra blank tubes containing only 1.0 mL of medium (no HA) were prepared. Next, all 8 tubes with samples were put on a test-tube rotator (Model LD79, Labinco BV, the Netherlands) and mixed at 5 rpm at room temperature for 30 min until homogenous dispersion was obtained. Lastly, the tubes were left in a vertical position at room temperature overnight for equilibration in order to achieve desorption of calcium and phosphate ions from HA surface.

Next day, the test-tube rotator was placed in the heating chamber at 35 °C. All test tubes were mixed at 5 rpm for 1 h in order to resuspend HA. The NP samples were also placed in the same heating chamber in order to be warmed them up to the same temperature before performing the adsorption experiment. In the next step, 2.0 mL of GF NPs were introduced into each test tube and mixed on the test-tube rotator for 5 min (20 rpm, 35 °C). All samples were centrifuged (Centrifuge 5430 R, Eppendorf, Germany) at 1,100 rpm for 10 min at room temperature. Finally, 1 mL samples of the supernatants were collected and transferred into 1.5 mL plastic Eppendorf tubes.

Throughout the whole experiment, samples were covered with aluminum foil due to FITC' photosensitivity. Quantification of NP samples was done as described in *Chapter 3.5.3*.

3.9 Interaction of Nanoparticles with Mucins

The interaction study of NPs with mucins was performed using GF FITC-labeled fluoride-loaded chitosan NPs.

To begin with, 0.5 %, (w/w), 0.25 % (w/w), and 0.125 % (w/w) mucin solutions were prepared. Phosphate buffer of pH 6.8 was used as a dispersion medium. Next, 2 mL aliquots of NP dispersion were introduced in 4 test tubes with stoppers. 0.5 mL of previously prepared mucin solutions with 3 different concentrations were added into each test tube. In the remaining 4^{th} test tube, 0.5 mL of phosphate buffer was added serving as a control. All 4

test tubes were put on a test-tube rotator (Model LD79, Labinco BV, the Netherlands) and mixed at 5 rpm at room temperature for 30 min until homogenous dispersion of NPs was obtained. Afterwards, they were centrifuged (Centrifuge 5430 R, Eppendorf, Germany) for 10 min at 1100 rpm at room temperature. Finally, 1 mL of the supernatants were collected and transferred into 1.5 mL plastic Eppendorf tubes.

Quantification of NP samples was done as described in *Chapter 3.5.3*.

4 RESULTS AND DISCUSSION

4.1 Formation of Nanoparticles

Pistone *et al.* have shown that the characteristics of the chitosan NPs can be greatly influenced by the preparation parameters, especially the concentration of the cross-linker (45). Moreover, the factors such as the polymer concentration, the pH of the dispersion medium and its ionic strength, the polymer's molecular weight, and the mixing and stirring conditions greatly affect NPs formation as well (46). In this study, Pistone *et al.* tested formulations with TPP-to-chitosan ratio 10:90, 15:85, 20:80 and 25:75 (w:w). They reported that chitosan NPs with TPP-to-chitosan ratio 20:80 (w:w) had the smallest average particle size, low PDI and monomodal size distribution among all formulations they had prepared. They attributed these advantageous particle characteristics to the formation of cross-links within the NPs that reduced the repulsive forces between the polymer chains. This resulted in particle contraction while increasing their compactness. Because of this, the above mentioned ratio was used in the process of preparation of polymeric NPs (45, 47).
With all that considered, the aim was to prepare chitosan NPs with composition specified in *Table V*.

***Table V**: Composition of chitosan NPs.*

	Compound	Final Content
Polymer	Chitosan	0.070 % (w/w)
Cross-linker	TPP	20:80 (w:w)*
API	NaF	0.2 % (w/w)
Dispersion medium	Milli-Q water	/

**Cross-linker-to-polymer ratio*

Measurements in *Table VI* show characteristics of the first samples of prepared chitosan NPs. NPs had low PDI values (~0.10) with monomodal size distributions and small average particle sizes (~145 nm). High derived count rate values and low attenuator indexes used in the measurement indicate high particle concentration in the samples. The pH of NP dispersions was close to neutral.

***Table VI**: Average diameter and PDI of chitosan NPs and pH of NP dispersions.*

Sample	Average Diameter [nm]	PDI	pH	Attenuator Index	Derived Count Rate [kcps]
1	146.4	0.12	6.95	6	121,445
2	147.7	0.09	6.91	6	123,641

Visual inspection of NP dispersions showed no visible aggregates nor flocculates. No sediment was observed as well. The particle dispersions were colorless and transparent.
Based on the results obtained, it can be concluded that the first experiments of chitosan NP preparation were successful.
In the next step, the aim was to prepare FITC-labeled chitosan NPs. Firstly, the attempt to prepare NPs from only fluorescently-labeled chitosan was made. While trying to filter solution of fluorescently-labeled chitosan through 0.8 μm sterile syringe filter (see *Chapter 3.2*), the chitosan–FITC solution was shown to be too viscous, since the syringe filter got clogged during the filtration. Therefore, only 5 % of FITC-labeled chitosan for preparation of fluorescently labeled NPs was used (*Table VII*).

***Table VII**: Composition of FITC-labeled chitosan NPs.*

	Compound	Final Content
Polymer	5 % (w/w) FITC–chitosan* 95 % (w/w) chitosan	0.070 % (w/w)
Cross-linker	TPP	20:80 (w:w)**
API	NaF	0.2 % (w/w)
Dispersion medium	Milli-Q water	/

** Chitosan labeled with fluorescein isothiocyanate (FITC)*
*** Cross-linker-to-polymer ratio*

The results from the characterization of the chitosan–FITC NPs are presented in *Table VIII*. As well as the non-FITC-labeled NPs, the chitosan–FITC NPs show small average particle diameters (~100 nm) and low PDI values (~0.14), indicating homogeneous particle size in the samples. Relatively high derived count rates show that the concentration of particles in the sample was high, but still lower than in samples prepared without FITC-

labeled chitosan. Average diameters were smaller which could be due to the fluorescently-labeled chitosan.

The pH of fluorescently-labeled NP dispersions was ~6.50. The incorporation of FITC-labeled chitosan could have had an effect on the decrease in pH value compared to the non-FITC-labeled NP dispersions. Moreover, the difference in pH could have played a role in the process of the NP formation, since pH has a crucial effect on chitosan ionization. During the process of particle formation, amino groups in chitosan–FITC were more protonated than amino groups in non-labeled chitosan and could have, therefore, formed more bonds with oppositely charged TPP. This could have increased particle compactness and yielded smaller NPs.

Based on the results obtained, it can be concluded that preparation of FITC-labeled chitosan NPs was successful.

***Table VIII**: Average particle diameter and PDI of chitosan–FITC NPs, and pH of chitosan–FITC NP dispersions.*

Sample	Average Diameter [nm]	PDI	pH	Attenuator Index	Derived Count Rate [kcps]
1	96.9	0.14	6.44	6	47,019
2	104.0	0.14	6.47	6	52,312

There were no aggregates nor flocculates observed in the NP dispersions. The particle dispersions were transparent and lightly orange colored due to the presence of FITC-labeled chitosan.

4.2 Effects of Purification by Gel-filtration on Nanoparticles

Gel-filtration is a chromatography technique that can be utilized to separate molecules or particles based on their size differences. Separation happens when molecules or particles of various sizes move through porous matrix to which they have different degree of access due to the steric reasons (48). Smaller molecules have better access, whereas larger molecules' access is more constrained. The aqueous buffer (the mobile phase) travels through chromatography column containing the matrix, enabling the separation.

- Molecules smaller than the largest pores infiltrate the pores of the matrix to the greater extent than the larger molecules due to the larger accessible column volume and, as a result, get more retarded (they elute after the large molecules).
- Molecules larger than the largest pores are not able to enter the porous matrix and are consequently eluted first i.e. in or just after the void volume.

PD-10 desalting columns containing Sephadex G-25 Medium were used in the present thesis. They are employed in broad range of applications such as buffer exchange, desalting, separation of small molecules from large molecules etc. The aim was to effectively separate fluoride-loaded NPs from unentrapped fluoride, polymers, unbound dye (FITC) and other impurities potentially present in the samples. It should be acknowledged that every sample applied to desalting column became diluted (dilution factor: 1.4).

***Table IX**: Media used in gel-filtration of various NP samples.*

Sample type	Elution medium	Additional medium
Chitosan NPs	Phosphate buffer, pH 6.8	/
Chitosan–FITC NPs	Phosphate buffer, pH 6.8	/
Chitosan–FITC NPs	Phosphate buffer, pH 6.8	Artificial saliva
Chitosan–FITC NPs	Acetate buffer, pH 5.5	/

Measurements presented in *Table X* show a comparison of characteristics between NGF chitosan nanoparticulate samples with GF chitosan NPs. 10 mM phosphate buffer with pH 6.8 as an elution medium was used.

Chitosan samples that were subject to gel-filtration (GF samples) show slightly smaller average particle sizes and polydispersity compared to NGF samples, suggesting that gel-filtration chromatography managed to eliminate some larger particles, thus making particle size distributions more monomodal (*Table X*).

The investigated samples were colorless and transparent. Visual inspection after gel-filtration showed no apparent changes. The sample was clear, transparent and without any visible aggregates or sediment. The sample was clear due to the low initial NP concentration (0.070 % (w/w) chitosan concentration) that was also subject to dilution with dilution factor 1.4 as a result of gel-filtration.

***Table X**: Comparison of characteristics of NGF and GF chitosan NPs. Elution medium: 10 mM phosphate buffer (pH 6.8).*

Sample	Average Diameter [nm]	PDI	pH	Attenuator Index	Derived Count Rate [kcps]
1 (NGF)	113.8	0.145	6.21	7	12,504
2 (NGF)	123.0	0.142	6.21	7	12,506
1 (GF)	108.4	0.100	6.98	7	15,670
2 (GF)	113.8	0.112	7.01	7	15,436

Next step was the gel-filtration of FITC-labeled chitosan NPs. Results are presented in *Table XI*. As mentioned in *Chapter 4.1*, the NGF nanoparticulate dispersion containing chitosan–FITC NPs was lightly orange colored due to the fluorescein dye bound to the chitosan chains. A phosphate buffer was used as an elution medium in the purification process.

***Table XI**: Comparison of characteristics of NGF and GF chitosan–FITC NPs. Elution medium: 10 mM phosphate buffer (pH 6.8).*

Sample	Average Diameter [nm]	PDI	Attenuator Index	Derived Count Rate [kcps]
1 (NGF)	104.8	0.180	8	7,216
2 (NGF)	114.8	0.201	8	7,266
1 (GF)	128.1	0.301	9	2,304
2 (GF)	133.6	0.267	9	2,363

The measurements of chitosan–FITC GF samples show a slight increase in the average particle size and higher PDI compared to NGF samples. These results were probably a consequence of using the phosphate buffer with pH 6.8 as an elution medium. Namely, the ionic composition of phosphate buffer could have changed the physical stability of NPs. Hence, the unwanted changes in average diameter and PDI occurred. Furthermore, the drop in derived count rate numbers as well as the increase in attenuator index suggest a

significant fraction of particles was either successfully removed by gel-filtration or, even more likely, these particles started to dissolve and thus were not detected by Zetasizer.

To conclude, it is evident that unbound FITC was efficiently removed from the FITC-labeled chitosan NP dispersion by gel-filtration. In fact, this was confirmed visually as well: the GF NP dispersion was not lightly orange colored compared to the sample prior GF. It was transparent, without any visible aggregates or sediment. For this reason, it can be concluded that the gel-filtration chromatography is an appropriate separation technique for removal of the free dye, such as FITC, from the FITC-labeled chitosan NP dispersion.

Next, the effect of gel-filtration on the characteristics of NPs after they had been introduced into artificial salivary fluid (the SAGF medium) was investigated. *Table XII* shows the characteristics of GF and NGF chitosan–FITC NPs in artificial salivary fluid. Firstly, when comparing NGF samples to GF, the average particle sizes are smaller in GF samples suggesting larger particles were removed from dispersion by GF.

***Table XII**: Comparison of characteristics of NGF and GF chitosan–FITC NPs in artificial saliva. Elution medium: 10 mM phosphate buffer (pH 6.8).*

Sample	Average Diameter [nm]	PDI	Attenuator Index	Derived Count Rate [kcps]
1 (NGF)	630.5	0.443	8	2,905
2 (NGF)	1262.7	0.495	8	5,364
1 (GF)	288.2	0.446	11	231
2 (GF)	343.7	0.385	11	246

Secondly, the derived count rate numbers of GF samples exposed to artificial saliva were lower than the ones recorded for NGF samples, indicating that there was a smaller number of dispersed particles in the GF samples.

In the measurements of GF samples attenuator index 11 was used, indicating that no signal was blocked in measurement due to the extremely low light scattering detected by a photon detector. In other words, the detected particle concentration was extremely low, hence the highest attenuator index was used. This indicates that most of particles in both GF samples was probably either filtered away or dissolved. Visually, no aggregation or sedimentation in NGF nor GF samples was noticed.

Lastly, the effect of an acidic elution medium (10 mM acetate buffer, pH 5.5) on the outcome of gel-filtration was investigated. Measurements are presented in *Table XIII.* The average particle sizes decreased after GF suggesting larger particles were eliminated and the polydispersity of the sample was also decreased from 0.367 to 0.185, thus the NP dispersion after GF was considered to be monodisperse. The NP dispersion color changed from orange to colorless after being GF.

***Table XIII**: Comparison of NGF chitosan–FITC NPs to GF chitosan–FITC NPs. Elution medium: 10 mM acetate buffer (pH 5.5).*

Sample	Average Diameter [nm]	PDI	Attenuator Index	Derived Count Rate [kcps]
1 (NGF)	219.1	0.367	6	80,273
1 (GF)	160.9	0.185	7	15,904

PD-10 desalting columns used for gel-filtration in this research proved to be appropriate and effective for elimination of larger molecules and unbound dye from particle dispersions. Considering the removal mechanism, we believe we also effectively removed potential impurities from the samples using PD-10 desalting columns.

4.3 Stability of Nanoparticles in the Artificial Salivary Fluid

Numerous synthetic salivary fluids have been used for *in vitro* interaction studies in odontology. Although these fluids have more or less the same composition as human saliva, the formulation of a fluid exactly resembling physiological properties of natural saliva is still not possible.

It has long been known that biological fluids present on the site of the drug administration, such as saliva, greatly influence the performance of the DDS. Considering all electrostatic interactions occurring during the process of NP formation, it can be assumed that the ionic strength and the pH of salivary fluid, as well as its electrolyte composition can have an effect on the stability of nanoparticulate system.

The instability of ionically cross-linked NPs can occur, resulting in NP aggregation, NP disintegration, and swelling or shrinking of the particles (45, 47). Colloid aggregation can occur due to the presence of oppositely charged multivalent ions that interact with NPs and form ionic bridges between them or as a result of weakening charge repulsions between the particles. Disintegration can occur as result of breaking the electrostatic bonds between polysaccharide and cross-linker. Additionally, shrinking and swelling of NPs depend on the variations in charge density: higher charge density in proximity of NPs results in enhanced swelling of NPs, which increases the frictional forces among moving particles and, in the end, leads to particle disintegration (49).

Gal *et al*. have examined nearly 60 artificial salivas in order to clarify the role of the compounds present in some *in vitro* tests (44). Based on the study, they developed their own composition of solution for testing the behavior of various biomaterials – the SAGF medium. The main advantage of the SAGF medium is that it provides the researchers with the ability to perform all thermodynamic calculations in it because all stability constants of its chemical compounds are available in the literature. Moreover, it resembles the characteristics of natural saliva with respect to the pH, ionic strength, the buffering capacity, and the concentrations of ionic components in it. On the other hand, the SAGF medium does not contain any compounds that would simulate the glycoproteins, which are responsible for viscosity of natural saliva. The reason for inadequate viscosity is current unavailability of a suitable material, which would simulate natural glycoproteins. The composition of SAGF medium is presented in *Table IV (Chapter 3.7*). For all the above reasons, the SAGF medium in the interaction experiments was used.

It must be noted, the use of the SAGF medium demands special attention because the solution should be supersaturated with carbon dioxide with respect to the air. Consequently, the solution was a subject to CO_2 gas leakage, which in turn increased the pH of the medium. Before each experiment, CO_2 gas had to be reintroduced into the solution by bubbling. This restored the solution original ionic strength.

Results of physical stability of NPs in artificial saliva are depicted in *Figure 11* and *Figure 12*. The error bars represent the minimal and maximal values, and the points without error bars have minimal and maximal values equal to or smaller than the size of the markers. *Figure 11* shows a sample of NPs that was not purified by gel-filtration, whereas *Figure 12* presents a sample that was GF. The first measurement was recorded 5 min after mixing the SAGF medium with NPs in order to achieve temperature equilibration of the test system.

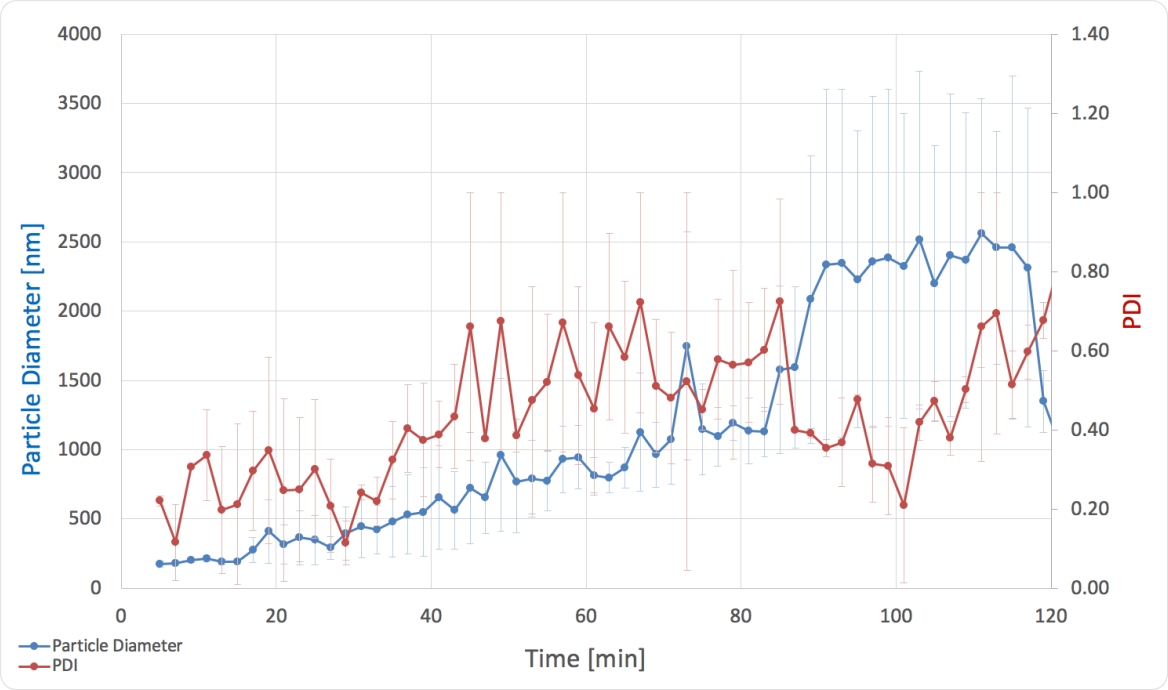

***Figure 11**: Changes of average NP diameter and PDI with time (NGF sample).*

The first particle size measurement revealed particle size of ~200 nm (*Figure 11* and *Figure 12*), which could indicate the beginning of NP aggregation immediately after contact with the artificial salivary fluid. Gradual increase in particles size and PDI in both investigated samples (*Figure 11* and *Figure 12*), as a function of time suggest particle aggregation with time. In two hours, the average particle size increased more than 8-fold, whereas PDI fluctuated in range from 0 to 0.80. *Figure 12* shows a decrease in the PDI at ~50 min mark. This is dissimilar from *Figure 11* that shows a decrease in the PDI at ~85 min mark. The error bars are long in *Figure 11*, but this can simply be due to the large particle sizes and the high PDI values.

The aggregation could be caused by interactions of NPs with multivalent anionic compounds of the SAGF medium (carbonates, sulfates, phosphates) which could interfere with positively charged particles. Apart from this, the presence of anions disrupted repulsive forces between nanoparticles by lowering overall nanoparticle charge, thus promoting aggregation. The increase in polydispersity (*Figure 11*) can be attributed to the formation of particle aggregates of various sizes.

Due to its hydrophilic properties and charged state, chitosan is susceptible to the pH changes of the medium. The pKa value of the chitosan is close to neutral pH (~6.5) consequently making its amino groups protonated in acidic medium. Contrary, chitosan particles

spontaneously form aggregates in medium with slightly basic pH, since they become uncharged. This can explain why aggregation occurs in the SAGF medium (pH 6.8), which, as mentioned before, tends to release CO_2 through time as a consequence of being supersaturated with CO_2 with respect to the air, thus becoming more alkaline, which could promote particle aggregation.

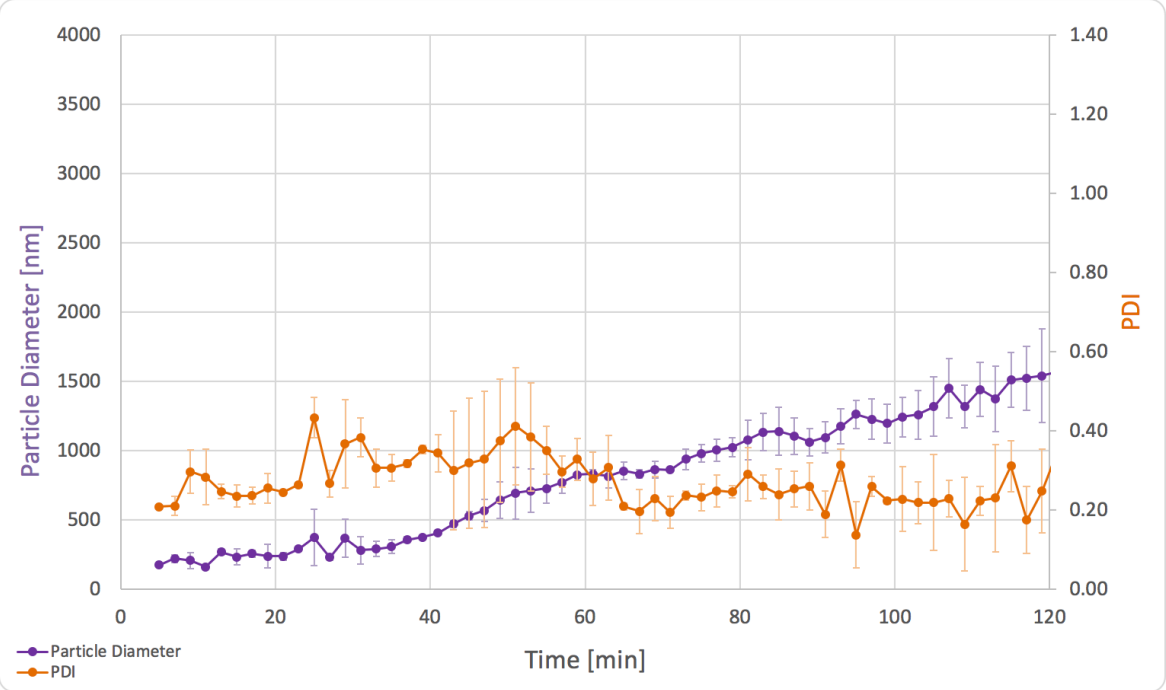

***Figure 12**: Changes of particle diameter and PDI with regard to time (GF sample).*

It should be acknowledged that the recorded derived count rates of measured samples never exceeded 7,000 kcps, indicating relatively low particle concentrations in all samples (*Figure 13*). The derived count rates rapidly increased and reached the peak value in the first three hours. This might have been due to rapid particle aggregation, that could have occurred in the first 180 min, when mixing of the particle dispersion with the artificial salivary fluid had been performed. Afterwards, the derived count rates started to decrease, which suggests that the process of particle disintegration was more pronounced than the process of particle disintegration. Additionally, the particle sedimentation contributed toward decrease in the derived count rates after 180 min had passed. After 300-minute mark, the disintegration rate slowed down to a point where it almost completely stopped, leading us to believe there were only small number of initial NPs left in the dispersion.

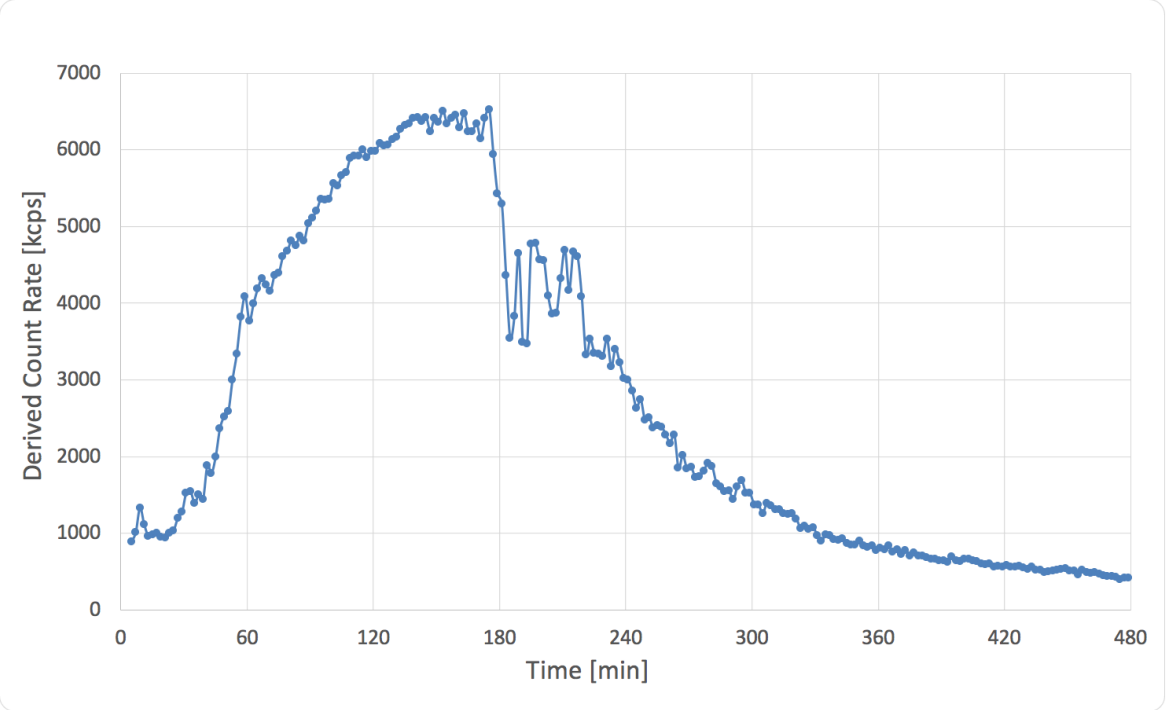

***Figure 13**: Derived count rates recordings for an NGF sample recorded over 8 h.*

To conclude, polysaccharide-based NPs proved to be extremely unstable in the presence of artificial saliva, which can be associated with particle aggregation and disintegration. Despite the fact that the SAGF medium is believed to be one of the most appropriate media to mimic all the aspects of the natural saliva, it is necessary to keep in mind that complexity and variability of natural saliva with regard to interactions that might be present can hardly be simulated *in vitro*. For that reason, further experiments employing different artificial saliva-mimicking media designed with other salivary components or even a use of natural saliva are required to gain a better understanding about behavior of the polymer-based nanosystems in an oral cavity.

4.4 Adsorption of Nanoparticles onto Hydroxyapatite Powder

The oral cavity is complex, versatile, and dynamic environment, especially due to the constant salivary flow which is responsible for a rapid clearance of delivered drug molecules. Apart from that, therapeutic agents administered to mouth in order to treat various mouth ailments such as bacterial or fungal infections and dental conditions, as caries and periodontal disease, are exposed to interactions with oral microorganisms, food components,

and mucosal epithelial cells. These interactions greatly affect drug residence time in the mouth and thereby shorten the duration of the drug effect. For this reason, special bioadhesive dosage forms with the ability to adhere onto oral tissues have been extensively researched and studied in the recent years (50, 51).

Most often, oral dosage forms are designed to target the buccal and the sublingual regions to achieve local or systemic effects. The treatment of dental problems with oral formulations has not been broadly explored. By adhering onto oral tissues, the retention time of pharmaceutical formulation would increase and thereby improve its local efficacy. Moreover, the polymers that have the capacity to adsorb onto the tooth surface could form a thin layer that could protect dental enamel from the acid erosion or cariogenic microorganisms, such as *Streptococcus mutans*, a significant contributor to tooth decay (52, 53).

In the present thesis, the adhesion capacity of polysaccharide nanosystem was evaluated by calculating the percentage of chitosan NPs adhered onto determined amounts of HA powder. The adsorption of NGF and GF chitosan NPs onto HA powder with respect to the amount of HA used to interact with NPs is shown in *Figure 14* and *Figure 15*. The points without error bars have minimal and maximal values equal to or smaller than the size of the markers.

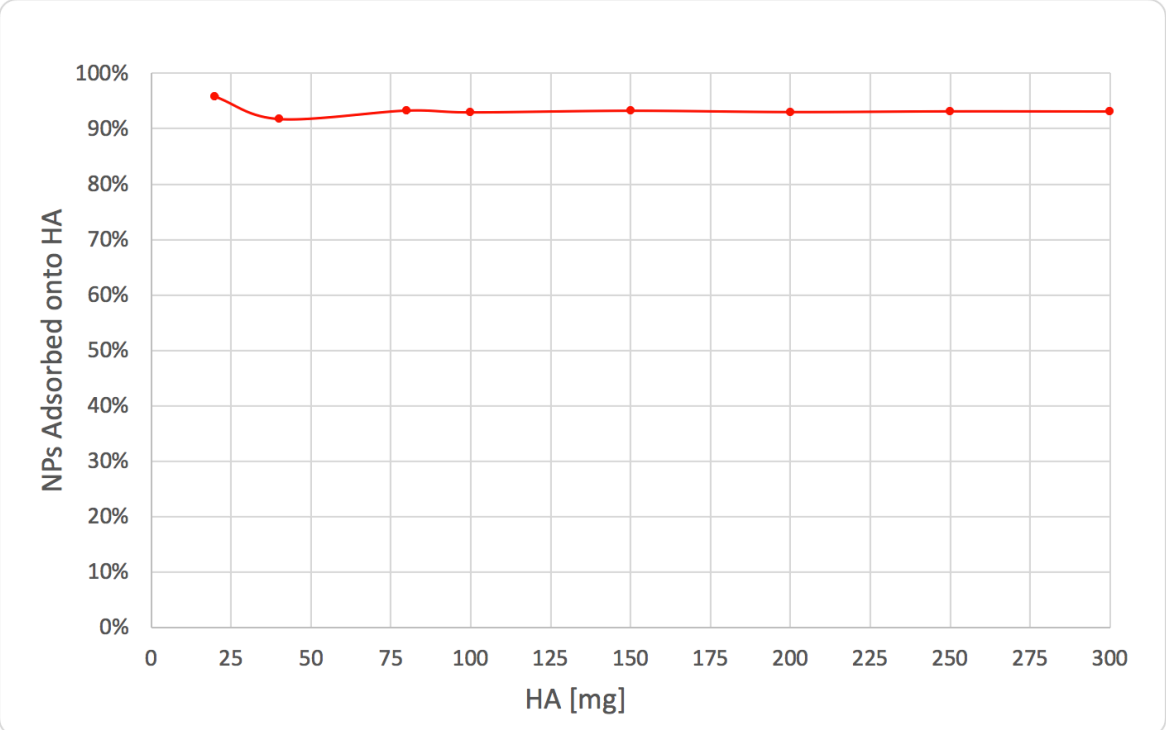

***Figure 14**: Adsorption of NGF FITC–chitosan NPs onto HA.*

All NGF samples (*Figure 14*) yielded extremely high fluorescence intensity levels that were closely matching 100 % fluorescence of blank samples (without any HA present) used to prepare a calibration curve. Therefore, the calculated NP adsorption onto HA always reached approximately 100 %, regardless to the amount of HA used. The graph indicates that the NP adsorption rate does not depend on the amount of HA the NPs interacted with. This can be attributed to unbound FITC molecules present in the samples that were detected by fluorescence spectroscopy, thus the obtained results are misleading.

On the contrary, varying fluorescence intensity levels of GF samples detected by fluorescence microscopy (*Figure 15*) suggest that the NP dispersion contained little or no unbound dye that could yield false positive results. *Figure 15* shows the percentage of NPs adsorbed onto HA powder, while keeping constant amount of NPs and increasing the amounts of HA. The adsorption percentage of NPs increased with respect to HA mass, until it reached a plateau value (~200 mg HA) at which all NPs were adsorbed onto HA.

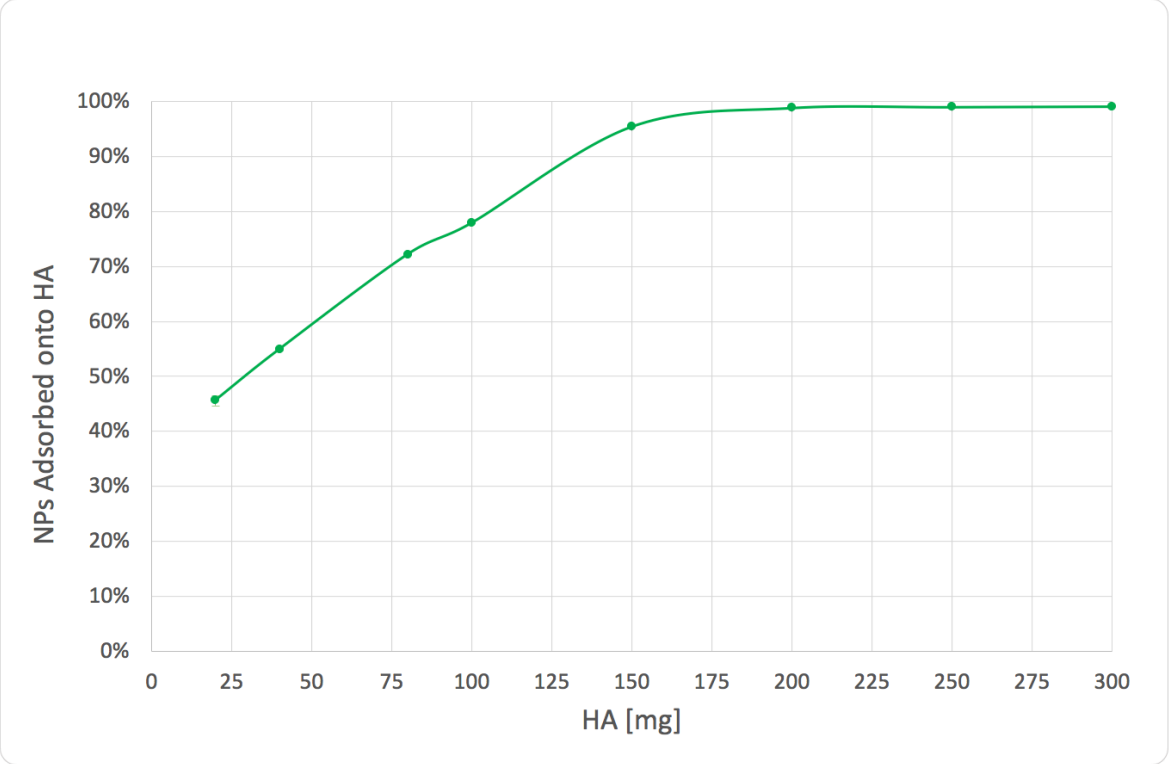

***Figure 15**: Adsorption of the chitosan NPs onto HA surface in 10 mM phosphate buffer (pH 6.8).*

Calcium hydroxyapatite ($Ca_5OH(PO_4)_3$) is commonly used as a model substance for dental enamel in bioadhesion research because it displays similar surface characteristics as the

dental enamel (54-56). Due to its amphoteric nature, the HA surface is capable of interacting with both cations and anions depending on pH of the medium. The process of adsorption and desorption involves two binding sites the HA shows: the positively charged calcium ions (Ca^{2+}) and negatively charged phosphate ions (PO_4^{3-}), which both form strong and non-specific electrostatic interactions with oppositely charged species. Nevertheless, in the presence of phosphate ions in phosphate buffer solution, the negative charge of the HA surface becomes more pronounced (47) and is consequently responsible for strong interactions with positively charged entities due to the electrostatic forces.

The adsorption of the NPs depends on the subtle balance between attractive and repulsive forces between NPs and the HA powder surface. The HA surface characteristics are greatly influenced by the pH, ionic strength and the concentration of various ions present in the surrounding environment (57). Phosphate ions present in the buffer used as an elution medium in gel-filtration chromatography are able to electrostatically adsorb onto HA and enamel surface in a dynamic equilibrium and, as a consequence, decrease the zeta potential of its surface. This can further increase the adsorption of the positively charged chitosan NPs onto HA. It has been reported that ions of different types, especially those present as components of saliva, as well as other salivary components affect the zeta potential of HA and enamel surface (57). However, the adsorption of chitosan NPs onto HA surface in the presence of artificial salivary fluid was not examined due to NP aggregation susceptibility in the presence of artificial saliva (see *Chapter 4.34.2*).

The adsorption of chitosan NPs onto HA and enamel could also be facilitated by the presence of TPP. To be more precise, TPP polyanions could act as bridges between HA surface, namely Ca^{2+} cations, and positively charged polymer chains. Hence, they promote the adhesion of chitosan NPs onto HA surface.

In order to simulate acidic conditions after oral microorganisms metabolize carbohydrates from food to lactic acid the adhesion experiment was performed with NPs purified by gel-filtration using acetate buffer (10 mM, pH 5.5) as an elution medium. The fluorescence intensity levels detected for samples proved to be too high to perform any further calculations to determine adsorption levels. After careful inspection, it became evident there were little to no particles present in the supernatant after centrifuging particle dispersion in presence of HA powder, as shown in *Table XIV*. This is indicated by significantly lower derived count rate number as well as high attenuator index used in measurements of supernatant with respect to NGF and GF samples. It is not possible to provide definite answers,

why that had occurred, however, it is reasonable to believe that the acetate buffer (pH 5.5) facilitated the disintegration of chitosan NPs during the centrifugation process. Namely, it is possible that the ionic components of acetate buffer interfered with intraparticle cross-links and destabilized particle structural integrity, which was not able to withstand the centrifugal forces.

***Table XIV**: Sample characteristics of chitosan–FITC NPs before gel-filtration, after gel-filtration, and after being centrifuged.*

Sample	Average Diameter [nm]	PDI	Attenuator Index	Derived Count Rate [kcps]
NGF	219.1	0.367	6	80,273
GF	160.9	0.185	7	15,904
Supernatant	528.0	0.533	11	317

During the FITC labeling of the polymer, some molecules of FITC remained unattached and were not removed by GF. These FITC molecules that were physically entrapped within the polymer chains might have been released and later detected by fluorescence spectroscopy in terms of extremely high fluorescence intensity values. It is also possible that there were some unbound FITC molecules present in the samples that had not been removed from the NP dispersion during purification by gel-filtration. These allegedly unbound FITC molecules could also contribute to detected high fluorescence intensity.

In the scope of measuring adsorption of NPs onto HA, the pH dependence of FITC fluorescence has also been investigated. The results shown in *Figure 16* are in line with results reported by Martin *et al* (58). Strong fluorescence of FITC is present in alkaline solutions, whereas lowering the pH reduces the fluorescence intensity. This can be attributed to the occurrence of different protolytic forms of the fluorescein that are a direct consequence of protolytic reactions in the excited state. The carboxyl group is susceptible to protonation and plays a major role in formation of a lactone (and cation) in acidic solutions. It has been suggested that depending on the pH, fluorescein may exist in form of cation, as neutral molecule, the lactone, the monoanion or the dianion *(Figure 17)*.

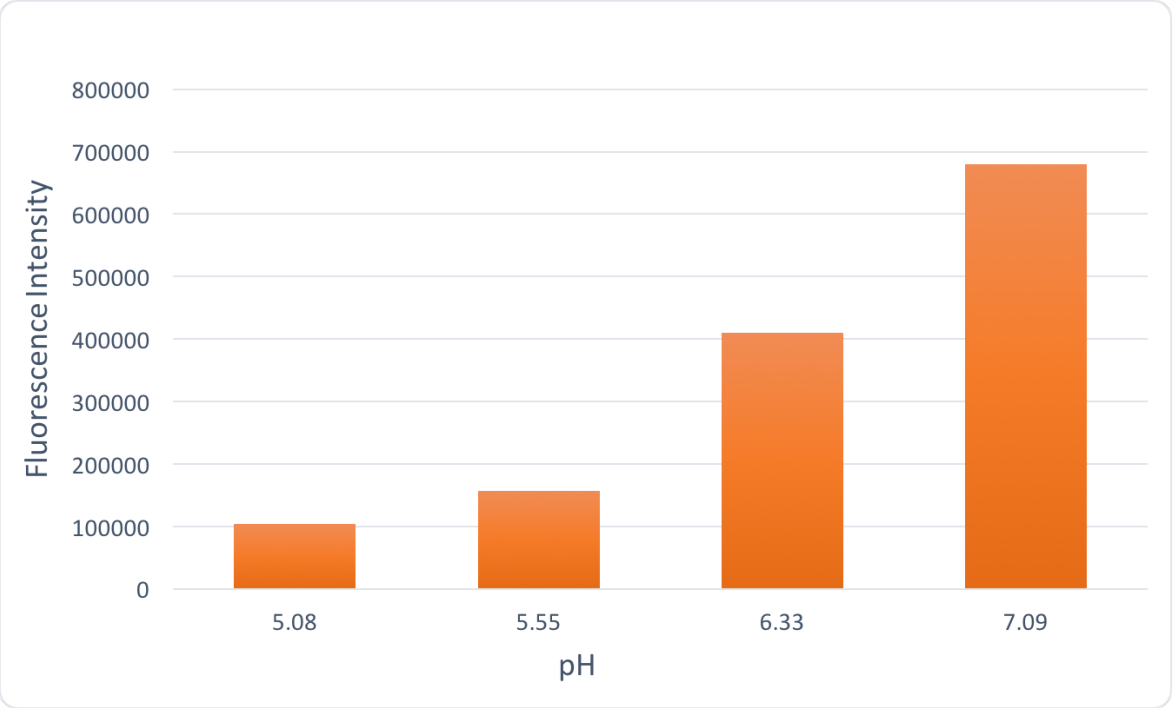

***Figure 16**: The fluorescence intensity of FITC solutions at various pHs.*

At each pH, one specific form of the dye predominates. Neutral FITC molecule exists partly as the lactone and partly as the neutral quinonoid molecule and has much lower absorption intensity than the other forms because the lactone does not absorb light in the visible spectrum. It has been reported only three different fluorescence absorption peaks are detected when pH is altered (58). In strongly acidic solutions, the cation emission occurs. At lower acidities, the emission can be akin to that of the neutral molecule. And lastly, in alkaline solutions, the strong dianion emission appears. For that reason, in solutions of various pH values, the measured fluorescence intensity varies with respect to acidity or alkalinity of the solution. This has also been observed and measured during the HA adsorption studies, as displayed in *Figure 16*.

This study was important because it paves the way for further experiments about the adsorption of NPs onto HA in different conditions, namely in media with different pHs.

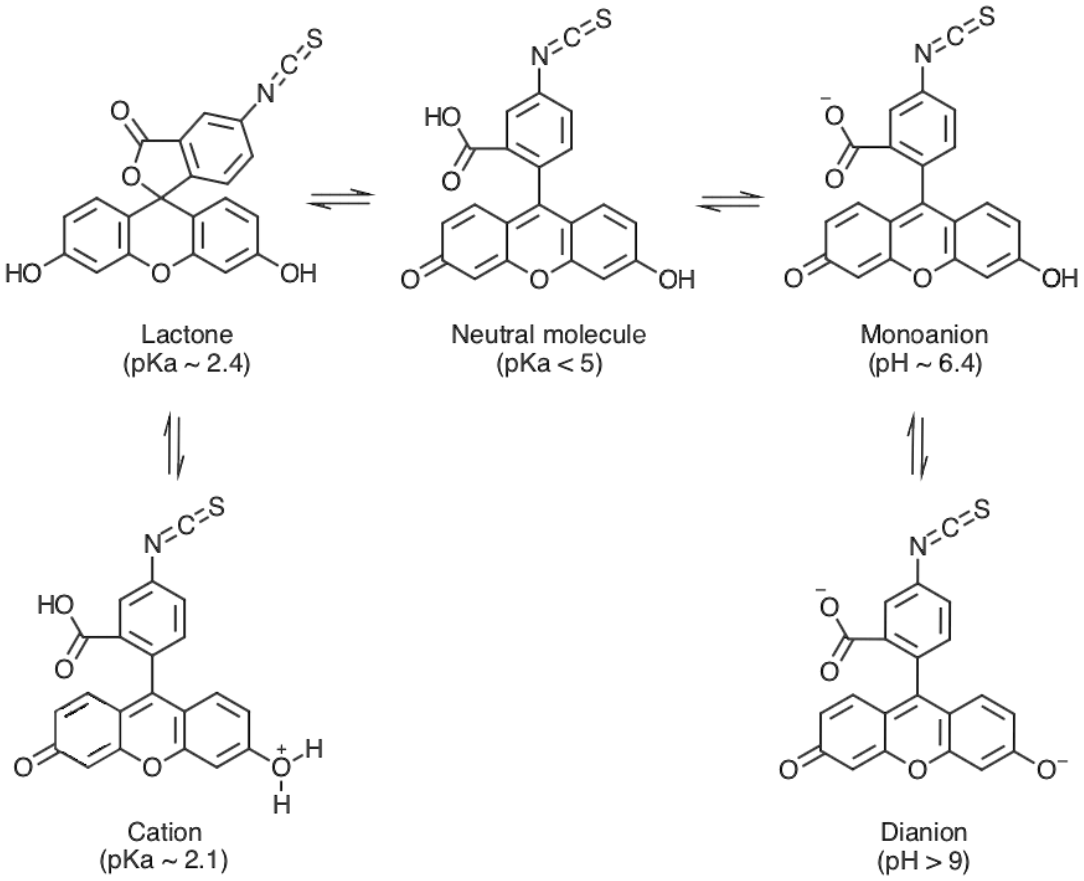

***Figure 17**: FITC in different predominating forms depending on the pH: the cation, the lactone, the neutral molecule, the monoanion and the dianion (58).*

4.5 Interaction of Nanoparticles with Mucins

In scope of the adsorption study of chitosan–FITC NPs a short experiment was performed in order to investigate the mucoadhesivity of chitosan NPs (*Figure 18*).

Over the years, mucoadhesive systems have been intensively studied as they provide a novel approach towards improving the performance of controlled-release DDS. Mucoadhesive polymers have the capacity to prolong retention of the formulation at the target site and thus improve API availability in terms of local or systemic therapy (59). In some cases, they even possess the ability to suppress enzymatic activity that could negatively impact the drug activity. Mucins are high molecular weight glycoproteins that are produced by mucosal epithelial cells. They constitute of subunits of various sizes that are interconnected through disulfide bonds. Their main characteristic is the ability to form a gel-like

layer over the mucosal epithelial cells, acting like a physicochemical barrier and protection barrier against pathogens (60).

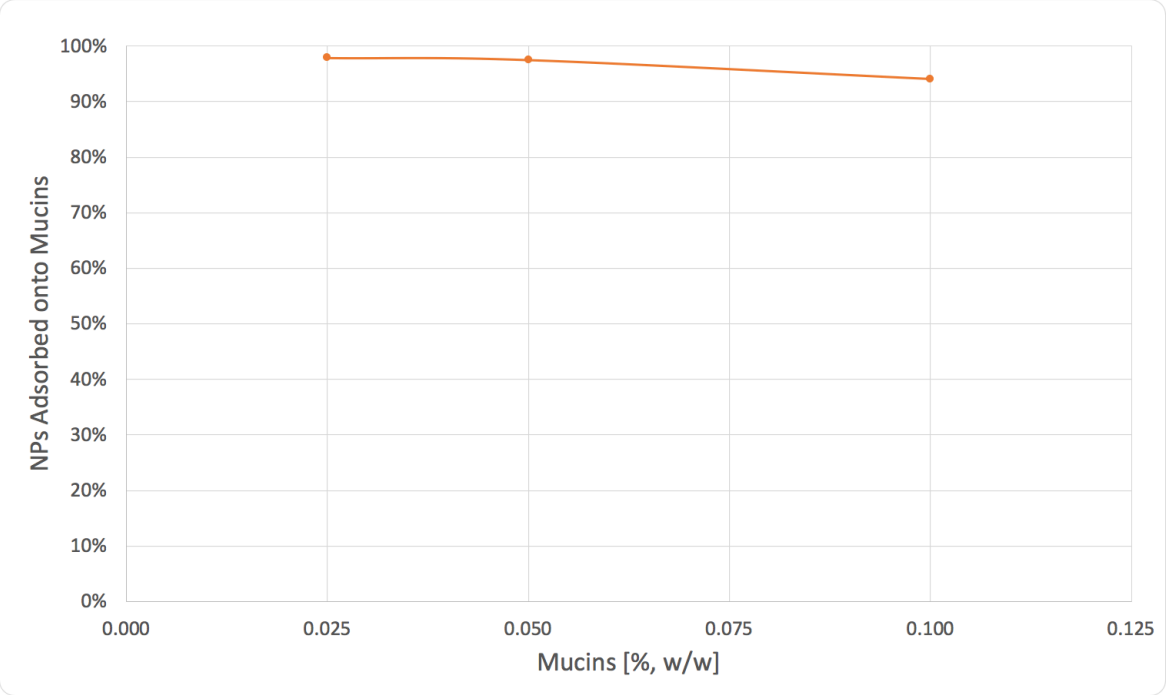

***Figure 18**: Interaction of the chitosan NPs with mucins in 10 mM phosphate buffer (pH 6.8) (n = 1).*

Figure 18 indicates that the percentage of NPs adsorbed onto mucins did not change significantly with respect to different mucin concentrations used. It has been previously suggested that more than one mucin molecule can bind and form interactions with each chitosan molecule. This might explain why this study showed relatively high percentage of NPs adsorbed onto mucins regardless to their concentration. It is very likely lower mucin concentrations would have shown a different result. There are no visible error bars in *Figure 18* because the error bars have minimal and maximal values equal to or smaller than the size of the markers.

In order to achieve the optimal mucoadhesion, the DDS' polymer chains should directly interact with the mucins. The interpenetration of polymer chains with mucin branches develops through diffusion and interlacing of the polymer chains. It is believed the primary attraction between polymer and mucosal molecules occurs due to the van der Waals forces, electrostatic interactions, hydrogen bonding or hydrophobic interactions (59). It has long been known that positively charged amino groups of chitosan bind to sialic acid residues of

mucins through the ionic interactions. All these interactions depend on the environmental pH and its ionic strength.

In light of the preliminary experiment it is reasonable to believe that chitosan NPs were able to adsorb onto mucins, thus they exhibit mucoadhesive properties. Despite that, additional research is required in order to provide more insights that would help us understand this phenomenon.

5 CONCLUSIONS

This research examined chitosan NPs loaded with fluoride. To be more specific, the main findings of this study are as follows:

1. Physically stable fluoride-loaded chitosan NPs were successfully prepared. The NPs had small average particle sizes (~145 nm) with monomodal size distributions (PDI ~0.100). The NP dispersions did not have any visible aggregates, flocculates, or sediment. They were colorless and transparent.

   The preparation of fluorescently-labeled fluoride-loaded chitosan NPs was successful. The NPs showed small average particle sizes (~100 nm) and homogeneous particle size distribution (PDI ~0.140). There were no aggregates nor flocculates observed in the NP dispersion. The NP dispersion right after preparation (NGF sample) was transparent and lightly orange colored due to presence of FITC-labeled chitosan.
2. Gel-filtration as a separation and purification method was demonstrated to be essential for removal of unbound fluorescent dye (FITC). Additionally, the removal of larger particles from NP dispersion was also achieved.
3. Chitosan-based NPs proved to be extremely physically unstable in presence of artificial salivary fluid, resulting in particle aggregation and disintegration promoted by ionic components of artificial saliva.
4. NPs proved to have adhesion capacity onto HA. The adsorption percentage of NPs gradually increased with increasing amount of HA, until it reached a plateau value (~200 mg HA) at which all NPs were adsorbed onto HA.
5. NPs showed ability to adsorb onto mucins. The percentage of NPs adsorbed onto mucins did not change significantly with increasing amount of mucins available.

6 REFERENCES

1. Petersen, P.E., et al., *The global burden of oral diseases and risks to oral health.* Bulletin of the World Health Organization, 2005. **83**(9): p. 661-669.
2. World Health Organization, *Sugars and dental caries*. 2017, World Health Organization.
3. Blaus, B. *Mouth Anatomy*. [png] [cited 2018 28 June]; Mouth Anatomy]. Available from: https://commons.wikimedia.org/w/index.php?title=File:Blausen_0653_MouthAnatomy.png.
4. Berkovitz, B.K., G.R. Holland, and B.J. Moxham, *Oral anatomy, histology and embryology*. 2016: Elsevier.
5. Buzalaf, M.A.R., et al., *Mechanisms of action of fluoride for caries control*, in *Fluoride and the oral environment*. 2011, Karger Publishers. p. 97-114.
6. Blaus, B. *Tooth Anatomy*. [png] [cited 2018 28 June]; Tooth Anatomy]. Available from: https://commons.wikimedia.org/w/index.php?title=File:Blausen_0863_ToothAnatomy_02.png.
7. Dawes, C., *What is the critical pH and why does a tooth dissolve in acid?* Journal-Canadian Dental Association, 2003. **69**(11): p. 722-725.
8. Featherstone, J. and A. Lussi, *Understanding the chemistry of dental erosion*, in *Dental erosion*. 2006, Karger Publishers. p. 66-76.
9. De Almeida, P.D.V., et al., *Saliva composition and functions: a comprehensive review.* J contemp dent pract, 2008. **9**(3): p. 72-80.
10. Zahradnik, R., E. Moreno, and E. Burke, *Effect of salivary pellicle on enamel subsurface demineralization in vitro.* Journal of dental research, 1976. **55**(4): p. 664-670.
11. Meurman, J. and J. Ten Gate, *Pathogenesis and modifying factors of dental erosion.* European Journal of Oral Sciences, 1996. **104**(2): p. 199-206.
12. Lee, H.-S., et al., *Chitosan adsorption on hydroxyapatite and its role in preventing acid erosion.* Journal of colloid and interface science, 2012. **385**(1): p. 235-243.
13. Unknown. *Schematic illustration of oral mucosa layers*. [png] [cited 2018 28 June]; Available from: https://commons.wikimedia.org/wiki/File:Oral_mucosa.png.
14. Collins, L. and C. Dawes, *The surface area of the adult human mouth and thickness of the salivary film covering the teeth and oral mucosa.* Journal of dental research, 1987. **66**(8): p. 1300-1302.
15. World Health Organization. *Oral health*. Oral health documents and publications 2012 [cited 2018 26 April]; Available from: http://www.who.int/oral_health/publications/factsheet/en/.

16. Silk, H., *Diseases of the mouth.* Primary care: Clinics in office practice, 2014. **41**(1): p. 75-90.

17. Chien, Y., *Novel drug delivery systems*. 1991: CRC Press.

18. Zupancic, S., et al., *Contribution of nanotechnology to improved treatment of periodontal disease.* Current pharmaceutical design, 2015. **21**(22): p. 3257-3271.

19. Vauthier, C. and K. Bouchemal, *Methods for the preparation and manufacture of polymeric nanoparticles.* Pharmaceutical research, 2009. **26**(5): p. 1025-1058.

20. Sanna, V., N. Pala, and M. Sechi, *Targeted therapy using nanotechnology: focus on cancer.* International journal of nanomedicine, 2014. **9**: p. 467.

21. Zhang, H., et al., *Design of biocompatible chitosan microgels for targeted pH-mediated intracellular release of cancer therapeutics.* Biomacromolecules, 2006. **7**(5): p. 1568-1572.

22. Mozafari, M., *Nanoliposomes: preparation and analysis*, in *Liposomes*. 2010, Springer. p. 29-50.

23. Qin, C., et al., *Water-solubility of chitosan and its antimicrobial activity.* Carbohydrate polymers, 2006. **63**(3): p. 367-374.

24. Rabea, E.I., et al., *Chitosan as antimicrobial agent: applications and mode of action.* Biomacromolecules, 2003. **4**(6): p. 1457-1465.

25. Cheung, R.C.F., et al., *Chitosan: an update on potential biomedical and pharmaceutical applications.* Marine drugs, 2015. **13**(8): p. 5156-5186.

26. Mahmoudian, J., et al., *Comparison of the photobleaching and photostability traits of Alexa Fluor 568-and fluorescein isothiocyanate-conjugated antibody.* Cell Journal (Yakhteh), 2011. **13**(3): p. 169.

27. Song, L., et al., *Photobleaching kinetics of fluorescein in quantitative fluorescence microscopy.* Biophysical journal, 1995. **68**(6): p. 2588.

28. Gan, Q., et al., *Modulation of surface charge, particle size and morphological properties of chitosan–TPP nanoparticles intended for gene delivery.* Colloids and Surfaces B: Biointerfaces, 2005. **44**(2): p. 65-73.

29. World Health Organization, *20th WHO Model List of Essential Medicines*, in *20th List*. 2017, World Health Organization. p. 49.

30. Vranic, E., et al., *Formulation ingridients for toothpastes and mouthwashes.* Bosn J Basic Med Sci, 2004. **4**(4): p. 51-8.

31. Friedman, A.J., et al., *Antimicrobial and anti-inflammatory activity of chitosan–alginate nanoparticles: A targeted therapy for cutaneous pathogens.* Journal of Investigative Dermatology, 2013. **133**(5): p. 1231-1239.

32. Jayakaran, T.G. and R. Arjunkumar, *Nanocomposite hydrogels as local drug delivery in periodontics.* 2013.

33. Gaumet, M., et al., *Nanoparticles for drug delivery: the need for precision in reporting particle size parameters.* European journal of pharmaceutics and biopharmaceutics, 2008. **69**(1): p. 1-9.

34. Petros, R.A. and J.M. DeSimone, *Strategies in the design of nanoparticles for therapeutic applications.* Nature reviews. Drug discovery, 2010. **9**(8): p. 615.

35. Soares, R.V., et al., *Salivary micelles: identification of complexes containing MG2, sIgA, lactoferrin, amylase, glycosylated proline-rich protein and lysozyme.* Archives of oral biology, 2004. **49**(5): p. 337-343.

36. Rykke, M., et al., *Micelle-like structures in human saliva.* Colloids and Surfaces B: Biointerfaces, 1995. **4**(1): p. 33-44.

37. Rajaonarivony, M., et al., *Development of a new drug carrier made from alginate.* Journal of pharmaceutical sciences, 1993. **82**(9): p. 912-917.

38. Huang, Y. and Y. Lapitsky, *Monovalent salt enhances colloidal stability during the formation of chitosan/tripolyphosphate microgels.* Langmuir, 2011. **27**(17): p. 10392-10399.

39. Berne, B.J. and R. Pecora, *Dynamic light scattering: with applications to chemistry, biology, and physics*. 2000: Courier Corporation.

40. Limited, M.I. *A basic guide to particle characterization*. 2015.

41. Nobbmann, U. *Derived count rate – what is it?* [Web page article] [cited 2017 13 September]; Available from: http://www.materials-talks.com/blog/2015/06/11/derived-count-rate-what-is-it/.

42. Hooijschuur, J.H. *Fluorescence spectroscopy*. Spectrometry (basics) [Web page article] 2018 [cited 2018 13 April]; Available from: http://www.chromedia.org/chromedia?waxtrapp=mkqjtbEsHiemBpdmBlIEcCArB&subNav=cczbdbEsHiemBpdmBlIEcCArBP.

43. Hof, M., V. Fidler, and R. Hutterer, *Basics of fluorescence spectroscopy in biosciences*, in *Fluorescence Spectroscopy in Biology*. 2005, Springer. p. 3-29.

44. Gal, J.-Y., Y. Fovet, and M. Adib-Yadzi, *About a synthetic saliva for in vitro studies.* Talanta, 2001. **53**(6): p. 1103-1115.

45. Pistone, S., et al., *Formulation of polysaccharide-based nanoparticles for local administration into the oral cavity.* Eur J Pharm Sci, 2017. **96**: p. 381-389.

46. Jonassen, H., et al., *Preparation of ionically cross-linked pectin nanoparticles in the presence of chlorides of divalent and monovalent cations.* Biomacromolecules, 2013. **14**(10): p. 3523-3531.

47. Pistone, S., *Formulation and evaluation of polysaccharide-and liposome-based nanosystems for improved targeting to the oral cavity.* 2016.

48. Hagel, L., *Gel-Filtration Chromatography*, in *Current Protocols in Molecular Biology*. 2001, John Wiley & Sons, Inc.

49. López-León, T., et al., *Physicochemical characterization of chitosan nanoparticles: electrokinetic and stability behavior.* Journal of Colloid and Interface Science, 2005. **283**(2): p. 344-351.

50. Gandhi, R.B. and J.R. Robinson, *Oral cavity as a site for bioadhesive drug delivery.* Advanced drug delivery reviews, 1994. **13**(1-2): p. 43-74.

51. Smart, J.D., *Recent developments in the use of bioadhesive systems for delivery of drugs to the oral cavity.* Critical Reviews™ in Therapeutic Drug Carrier Systems, 2004. **21**(4).

52. Churchley, D., et al., *Fluoropolymers as low-surface-energy tooth coatings for oral care.* International journal of pharmaceutics, 2008. **352**(1): p. 44-49.

53. Beyer, M., et al., *Pectin, alginate and gum arabic polymers reduce citric acid erosion effects on human enamel.* Dental Materials, 2010. **26**(9): p. 831-839.

54. Nguyen, S., et al., *The influence of liposomal formulation factors on the interactions between liposomes and hydroxyapatite.* Colloids and Surfaces B: Biointerfaces, 2010. **76**(1): p. 354-361.

55. Moreno, E.C., M. Kresak, and D.I. Hay, *Adsorption of molecules of biological interest onto hydroxyapatite.* Calcified Tissue International, 1984. **36**(1): p. 48.

56. Carlén, A., et al., *Bacteria-binding plasma proteins in pellicles formed on hydroxyapatite in vitro and on teeth in vivo.* Molecular Oral Microbiology, 2003. **18**(4): p. 203-207.

57. Yin, G., et al., *Impacts of the surface charge property on protein adsorption on hydroxyapatite.* Chemical Engineering Journal, 2002. **87**(2): p. 181-186.

58. Martin, M.M. and L. Lindqvist, *The pH dependence of fluorescein fluorescence.* Journal of Luminescence, 1975. **10**(6): p. 381-390.

59. Qaqish, R. and M. Amiji, *Synthesis of a fluorescent chitosan derivative and its application for the study of chitosan–mucin interactions.* Carbohydrate Polymers, 1999. **38**(2): p. 99-107.

60. Marin, F., et al., *Molluscan shell proteins: primary structure, origin, and evolution.* Current topics in developmental biology, 2007. **80**: p. 209-276.